

Dear Dr. Blöschl:

Thank you for your comments. We had previously revised the paper but we were unable to upload it when we uploaded the original response to the referees' comments. However, we have made further changes, described below, and have now been able to upload the revised manuscript.

We look forward to hearing from you regarding the revised manuscript.

Sincerely,
Dorothy Hall

Please note that the blue bold font represents today's response, and the black bold font is copied and pasted from our earlier responses. Referees' comments are in non-bold black font.

We have softened and toned down the following statement: "We conclude that the MODIS Terra CGF is the more accurate MODIS snow-cover product." In the revised paper that we've uploaded, we have restated that as follows in the Abstract: According to our preliminary validation of the Terra and Aqua MODIS CGF SCE products in the western U.S. study area, we found higher accuracy of the Terra product as compared to the Aqua product. The MODIS CGF snow-cover time series may be used to extend the SCE data record from 2000, into the VIIRS era through the early 2030s and perhaps beyond.

In our response to the referees' comments that we had previously uploaded, we responded to comments #5 and #6 of Referee #1, and also the question about validation of snow depth posed by Referee #2. Our original responses are provided below in black font. Additional comments in response to your queries are shown in blue font.

From Reviewer #1's review:

5) Why only temporal filter is considered for gap-filling method? During snowmelt, snow-line approach or some kind of spatial filter can be more efficient.

Authors: There are many other useful methods of gap filling, but the method described in our paper is the method that is used to develop the new product that will be available starting this summer or fall. We are beyond the point where different methods can be considered since the new algorithm uses the CGF method, all of the programming has been completed by the MODIS Project and the products will be available soon. It is too late to change the algorithm for Collection 6.1.

There is no doubt that other methods of gap filling are useful and perhaps even more accurate or efficient than the method used in the NASA standard MODIS CGF product. However the method selected, as described in Hall et al. (2010) and Riggs et al. (2017b), cannot be changed because the CGF product is "in production."

Therefore we do not understand why Referee #1 wants us to compare gap-filling methods beyond saying that there are some very good methods out there that differ from the method that we've selected. Several years ago we selected one method based on the fact that we must produce the product very quickly after data acquisition. For example, we don't have the luxury of waiting until the clouds clear after the day in question and then looking back to fill in gaps caused by clouds. We needed an algorithm that produces a snow map within a few hours after data acquisition and we settled on the CGF algorithm described in this paper. That was decided and approved by the MODIS Project several years ago. We cannot change it now.

6) The results show only few examples which does not allow to see clearly if the results are robust and general. More thorough analysis (longer time periods, seasonal evaluation, larger/different regions) will allow to draw much more robust findings.

Authors: We agree with this comment, but we are unable to do a thorough and global analysis because the product is not yet being produced by the MODIS and VIIRS Projects. When processing starts, the product will be downloadable through the National Snow and Ice Data Center starting in the fall of 2019.

In order to develop a time series in this pre-production phase, we need to do a considerable amount of programming. We've done this by developing a Terra MODIS CGF SCE time series for the western U.S. data set for 2012. For this revised version of the paper, and in response to this and other comments, we ran a 3-month time series using VIIRS SCE maps (see Figure 9). Running a CGF time series is computationally burdensome, and therefore a comprehensive, global analysis cannot be accomplished until after the official MODIS processing begins. Even after production begins it will take many months until the complete MODIS and VIIRS time series (from 2000 to present for MODIS and from 2011 to present for VIIRS) can be processed. Complete processing is likely to occur sometime in the year 2020 for both the MODIS C6.1 and VIIRS C2 CGF SCE products.

Recently we found out that MODIS data processing of Collection 6.1, that includes producing the CGF snow product, will begin by early October 2019. It may take up to one year to process all of the data, globally, from 2000 – present. Until processing has been completed near the end of the year 2020, we cannot do comprehensive global validation.

In short, processing will not be complete in a time frame that is reasonable for providing the revisions to this paper. And it is important that this paper be published so that users of the new products will have the information contained in this paper when the products first become downloadable from NSIDC in the fall of 2019. After processing has been completed, global validation will be possible by users globally. Comprehensive global validation is not something that is possible for one person or one small group to complete.

Additionally, VIIRS data processing is not likely to start until later this fall. Therefore it won't be possible to even begin validating the VIIRS CGF snow products probably until early 2020. Again, many months will be required for the NASA VIIRS Project to fully process the VIIRS time series (2011 – present).

Comment from the editor that Reviewer #2's comment about global validation was not addressed adequately:

I agree that validation of the satellite data is only possible by comparison with measurements. The manuscript presents validation against the NOAA snow depth data provided by the dense network of meteorological stations. Such networks are not available in other countries. Can we trust that the CGF maps are valid also in those parts of the world where the network density does not allow detailed validation?

Our original response is shown below. Additional comments are shown in blue.

Authors: Evaluation of the CGF maps in other countries will have to wait until the products are released and available to download through NSIDC (beginning in the fall of 2019). In areas of the world where the network of meteorological stations is not dense enough to allow validation, there are other methods to evaluate the uncertainties. These methods, discussed in the paper, include comparison with other snow maps, comparison with higher-resolution satellite data (such as with Landsat or Sentinel data), and comparison with surface reflectance maps such as from MODIS and VIIRS.

The MODIS SCE products have been validated and evaluated in many regions of the world; there are numerous peer reviewed articles published on this topic. However, the VIIRS SCE daily tiled product has not yet been released; only the swath product is available, so evaluation research has not yet appeared in the literature because users tend to be more comfortable using a tiled product than a swath product. In our comparisons between MODIS and VIIRS CGF products we have found very good agreement between MODIS and VIIRS SCE and CGF products thus there is the expectation that the VIIRS products will have similar accuracy to that reported for MODIS. We acknowledge, however, that the comparisons are necessarily limited because product production has not yet begun.

It is incumbent on the user to validate the product in his/her study area. While we, the product developers, can do preliminary validation, we cannot perform global validation. For one thing we are not as knowledgeable about snow-covered areas on different continents and in different countries as are the researchers who live there.

Evaluation of MODIS and VIIRS Cloud-Gap Filled Snow-Cover Products for production of an Earth Science Data Record: Advantage and Uncertainties

Dorothy K. Hall^{1,2,3}, George A. Riggs^{2,3,4}, Nicolo E. DiGirolamo^{2,3,4} and Miguel O. Román^{4,5}

¹Earth System Science Interdisciplinary Center, University of Maryland, College Park, MD 20740, USA

²Cryospheric Sciences Laboratory, NASA / Goddard Space Flight Center, Greenbelt, MD 20771, USA

³~~Under contract to SSSAI, Lanham, MD 20706, USA~~

^{3,4}SSAI, Lanham, MD 20706, USA

^{4,5}Earth from Space Institute / USRA, 7178 Columbia Gateway Dr., Columbia, MD 21046, USA

Correspondence to: Dorothy K. Hall (dkhall1@umd.edu)

Abstract. MODERate resolution Imaging Spectroradiometer (MODIS) cryosphere products that have been available since the launch of the Terra MODIS in 2000 and the Aqua MODIS in 2002 include [global snow-cover extent \(SCE\)](#) (swath, daily and eight-day composites) [at 500 m and ~5 km spatial resolution and daily snow albedo](#). These products are used [extensively](#) in hydrological modeling and [climate studies of local and regional climate, and are increasingly being used to study augment studies of regional hydrological and climatological changes over time](#).

Reprocessing of the complete snow-cover data record, from Collection 5 (C5) to Collection 6 (C6) and Collection 6.1 (C6.1), has ~~led to~~[provided](#) improvements in the MODIS product suite. Suomi National Polar-orbiting Partnership (S-NPP) Visible Infrared Imaging Radiometer Suite (VIIRS) Collection 1 (C1) ~~snow-cover products at 375 m spatial resolution~~ have been available since 2011, and are currently being reprocessed for Collection 2 (C2).

[Both the MODIS C6.1 and the VIIRS C2 products will be available to download through the National Snow and Ice Data Center beginning in the fall of 2019, with the complete time series available in 2020.](#) To address the need for a

cloud-reduced or cloud-free daily ~~sn~~[snow-SCE](#) product for both MODIS and VIIRS, a ~~new~~ daily cloud-gap filled (CGF) snow-cover ~~product algorithm~~ was developed for MODIS C6.1 and VIIRS C2 processing. MOD10A1F (Terra) and MYD10A1F (Aqua) are daily, 500-m resolution ~~cloud-gap-filled (CGF) snow-cover SCE~~ map products from MODIS. VNP10A1F is the ~~daily~~, 375-m resolution CGF ~~sn~~[snow-cover SCE](#) map ~~product~~ from VIIRS. ~~The~~[se](#) CGF ~~maps products provide daily cloud-free snow maps, along with include~~ quality-assurance data ~~such as including~~

cloud-persistence ~~maps statistics~~ showing the age of the ~~sn~~[snow or non snow](#) observation in each pixel. ~~The objective of this paper is to introduce the new MODIS and VIIRS standard CGF daily SCE products and to provide~~

~~preliminary evaluation of uncertainties in the gap-filling methodology so the products can be used as the basis for a moderate-resolution Earth Science Data Record (ESDR) of SCE. The objective of this paper is to introduce the new~~

~~MODIS and VIIRS standard CGF daily SCE products and to provide preliminary evaluation of uncertainties in the products so the products can be used as the basis for a moderate-resolution Earth Science Data Record (ESDR) of~~

~~SCE. SCE provide preliminary of from the CGF products, moderate resolution SCE. Work is ongoing to evaluate and document uncertainties in the MODIS and VIIRS standard daily CGF snow cover products. In this work, we~~

Formatted: Font color: Auto

Formatted: Font color: Auto, Strikethrough

Formatted: Strikethrough, Not Highlight

Formatted: Not Highlight

Formatted: Font color: Auto

42 ~~developed MODIS and VIIRS time series of the MODIS and VIIRS CGF products and have been developed and~~
43 ~~evaluated those time series in selected study sites in the United States U.S. and southern Canada. Analysis of the~~
44 ~~MOD/MYD10A1F product accuracies for study areas in the western United States shows excellent results in terms~~
45 ~~of accuracy of snow cover mapping. When there are frequent clear sky episodes, MODIS is the satellite~~
46 ~~instruments are able to capture enough clear views of the surface to produce accurate useful snow cover information~~
47 ~~and snow maps. Even in the extensively cloud covered northeastern United States during winter months, snow~~
48 ~~maps from MODIS CGF products are useful, though the snow maps are likely to miss some snow, particularly~~
49 ~~during the spring snowmelt period when snow may fall and melt within a day or two, before the clouds clear from~~
50 ~~the storm that deposited the snow. A time series comparison of three months of Terra MODIS and S-NPP VIIRS~~
51 ~~CGF snow cover maps, xx-xx, 2012, reveals xxx. Comparisons between the Terra and Aqua CGF snow cover~~
52 ~~maps The Observed differences, though small, have revealed differences that are related to are largely attributed to~~
53 ~~differences in cloud masking in the two algorithms and also differences in time of day of image acquisition.~~
54 ~~A However, a nearly three-month time-series comparison of Terra MODIS and S-NPP VIIRS CGF snow-cover maps~~
55 ~~for a large study area covering all or parts of 11 states in the western United States and part of southwestern Canada~~
56 ~~reveals excellent correspondence between the Terra MODIS and S-NPP VIIRS products, with a mean difference of~~
57 ~~11,070 km² for a large (~2,487,610 km²) which is ~0.45 percent of the study area in the western U.S. that includes~~
58 ~~all or parts of 11 states and part of southwestern Canada. We conclude According to our preliminary validation of the~~
59 ~~Terra and Aqua MODIS CGF SCE products in the western U.S. study area, wWe also e Additionally, we found that t~~
60 ~~that the higher accuracy of the Terra product MODIS CGF is the more accurate than as compared to the Aqua~~
61 ~~MODIS snow cover product, product. The MODIS CGF snow cover time series and should therefore form be the~~
62 ~~basis of an Environmental Science Data Record ESDR that will may be used to extend the CGF SCE data record~~
63 ~~from the Terra MODIS beginning in 2000, through into the VIIRS era, at least through the early 2030s and perhaps~~
64 ~~beyond.~~

Formatted: Font color: Auto

65
66 **1 Introduction**

67
68 Regular snow-cover mapping of the Northern Hemisphere from space began in 1966 when the National Oceanic and
69 Atmospheric Administration (NOAA) ~~began started~~ producing weekly snow maps to improve weather forecasting
70 (Matson and Wiesnet, 1981). A 53-year climate-data record (CDR) of Northern Hemisphere snow-cover extent
71 (SCE), based on NOAA's snow maps is ~~now~~ available at the Rutgers University Global Snow Lab (Robinson et al.,
72 1993; Estilow et al., 2015) ~~at a resolution of 25 km². Since the 1960s, snow cover mapping from space has become~~
73 ~~increasingly sophisticated. Not only has the temporal resolution of the NOAA snow maps increased from weekly to~~
74 ~~twice-daily, but the spatial resolution has also improved over time. Furthermore, dData from multiple satellite~~
75 ~~platforms and instruments with visible/near infrared (VNIR) and short wave infrared (SWIR) bands are now~~
76 ~~available to support improved snow mapping and snow/cloud discrimination as compared to the earliest satellite~~
77 ~~snow cover maps when sparse satellite data were available.~~

79 ~~Using the~~ Due to increasing global temperatures, especially in more northerly areas in the Northern Hemisphere, the
80 Rutgers CDR, ~~has been used by~~ researchers ~~for decades, and in recent years to show~~ have shown that SCE has been
81 declining and melt has been occurring earlier in the Northern Hemisphere (e.g., Déry and Brown, 2007). This
82 shortening of the snow season has many implications such as, for example, in the western United States (Mote et al.,
83 2005; Stewart, 2009; Hall et al., 2015), with earlier snowmelt contributing to a longer fire season (Westerling et al.,
84 2006; O’Leary et al., 2018) and other environmental and societal problems. However, the coarse resolution of the
85 Rutgers CDR is not suitable for regional and basin-scale studies.

86
87 Meltwater from mountain snowpacks provides hydropower and water resources to drought-prone areas such as the
88 western United States. Accurate snow measurement is needed as input to hydrological models that predict the
89 quantity and timing of snowmelt during spring runoff. SCE can be input to models to estimate snow-water
90 equivalent (SWE) which is the quantity of most interest to hydrologists and water management agencies.
91 Increasingly accurate predictions save money and water because reservoir management improves with
92 measurement accuracy knowledge of SWE improves increases.

93
94
95 Moderate medium-resolution SCE maps are produced daily from multiple satellite sensors such as ~~from~~ are on the
96 MODERate-resolution Imaging Spectroradiometer (MODIS) on both the Terra, ~~launched in 1999~~ launch), and
97 Aqua (~~launched in 2002~~ launch), ~~and satellites, and from~~ the Visible Infrared Imaging Radiometer Suite (VIIRS)
98 on the Suomi - National Polar Partnership (S-NPP) and the Joint Polar Satellite System – 1 (JPSS-1) satellites,
99 launched in 2011 and 2017, respectively. ~~These~~ snow maps from MODIS, in particular, are used extensively by
100 modelers and hydrologists to study regional and basin-scale ~~local~~ SCE and to develop snow-cover depletion curves
101 for multiple hydrological and climatological applications. Algorithms utilizing data from the VIIRS and MODIS
102 sensors provide global swath-based snow-cover maps with at spatial resolutions ranging from 375 m to 500 + km
103 under clear skies. Instruments on the Landsat series of satellites for which the record began in 1972, and other
104 higher-resolution sensors, such as from the more-recent Sentinel series, provide still-higher spatial resolution data
105 from which snow maps can be developed, though lower temporal resolution.

106
107 Cloud cover is the single most-important factor affecting the ability to map SCE accurately using visible and near
108 infrared (VNIR) and short-wave infrared (SWIR) sensors. Clouds ~~often frequently~~ create daily gaps in snow-
109 cover SCE maps that are generated using data only from VNIR and SWIR sensors. Cloud-gap filling can be used to
110 mitigate the cloud issue using VNIR and SWIR sensors. Additionally, ~~many~~ though useful, methods to combine
111 passive-microwave snow-cover maps with VNIR maps to eliminate clouds have been developed are only partially
112 successful (e.g., see Foster et al., 2011) but there are substantial limitations to the resulting products even though the
113 passive-microwave sensors can provide images through cloud cover. One way to mitigate the cloud issue is
114 through cloud-gap filling can be used to mitigate the cloud issue using VNIR and SWIR sensors (CGF).

Formatted: Font color: Auto

Formatted: Font color: Blue

116 In this paper, we describe the Terra and Aqua MODIS ~~and the S-NPP VIIRS cloud-gap filled (CGF) CGF~~
117 ~~algorithm~~ SCE map products have been developed to address the ~~cloud-gap~~ issues caused by gaps in data from cloud
118 cover when using VNIR and SWIR sensors, ~~data products and uncertainties~~. ~~These are new products that have not~~
119 ~~previously been available.~~ ~~Also discussed are advantages and uncertainties of the CGF SCE products from~~
120 ~~MODIS and VIIRS.~~ In addition to the inherent uncertainties in the MODIS snow maps, discussed elsewhere (e.g.,
121 Hall and Riggs, 2007, and in many numerous other papers), there are additional uncertainties related to gap filling
122 ~~that are addressed herein.~~ We also discuss the development of a moderate-resolution Environmental Science Data
123 Record (ESDR) of SCE and using MODIS and VIIRS standard snow cover maps. JPSS launches containing VIIRS
124 sensors are planned through at least 2031, continuing the SCE record at moderate spatial resolution.

125
126 ~~The objective of this paper is to introduce the new MODIS and VIIRS standard CGF daily SCE products and to~~
127 ~~provide preliminary evaluation of uncertainties in the gap-filling methodology so that SCE from the CGF the~~
128 ~~products can be used as the basis for a moderate-resolution Earth Science Data Record (ESDR) of SCE. seA~~
129 ~~thorough analysis of the uncertainties of these new products globally will not be possible until only after the entire~~
130 ~~time series have of both MODIS and VIIRS have been processed and archived which is likely to occur sometime in~~
131 ~~2020. The objective of this paper is to introduce readers to the new MODIS and VIIRS standard CGF daily snow~~
132 ~~cover products and to identify methods to evaluate and document uncertainties in the products. A thorough analysis~~
133 ~~of the uncertainties is not possible until all of the product time series has been processed and archived which is~~
134 ~~likely to occur sometime in 2020.~~

136 2 Background

138 2.1 Terra and Aqua MODIS

139
140 The MODIS instruments have been providing daily snow maps at a variety of temporal and spatial resolutions
141 beginning on 24 February 2000 following the 18 December 1999 launch of the Terra spacecraft ~~using a subset of the~~
142 ~~36 channels available on the MODIS sensors.~~ A second MODIS was launched on 4 May 2002 on the Aqua
143 spacecraft ~~and the data record began on 4 July n xx xxxx 2002.~~ The MODIS sensors ~~provide allowed the~~
144 ~~development of a large suite of land, atmosphere, and ocean products [https://modis.gsfc.nasa.gov], including daily~~
145 ~~maps of global snow cover and sea ice.~~ The prefix, MOD, refers to a Terra MODIS algorithm or product and MYD
146 refers to an Aqua MODIS algorithm or product. When the discussion in this paper refers to both the Terra and Aqua
147 products ~~it will be designated as such using we will use~~ the M*D nomenclature. Information on the full MODIS
148 standard cryosphere product suite is available elsewhere [https://modis-snow-ice.gsfc.nasa.gov/].

149
150 Since the launches of the Terra and Aqua spacecraft, there have been several reprocessings of the entire suite of
151 MODIS Land Data Products [https://modis-land.gsfc.nasa.gov/]. ~~Specifically~~ ~~In recent years,~~ reprocessing from
152 Collection 5 (C5) to Collection 6 (C6) and ~~in the near future,~~ Collection 6.1 (C6.1), has ~~led to been accomplished to~~

Formatted: Font color: Auto

Formatted: Font color: Auto

Formatted: Strikethrough

Formatted: Font color: Auto

Formatted: Font: Bold

Formatted: Font color: Auto

153 provide improvements in the MODIS snow-cover standard data products [to the user community](#) (Riggs et al., 2017a
154 and 2018).

155
156 A great deal of validation has been conducted on the MODIS snow-cover products through the C5 era (e.g., Klein
157 and Barnett, 2003; Parajka and Blöschl, 2006; Hall and Riggs, 2007; Frei and Lee, 2010; Arsenault et al., 2012 and
158 2014; Parajka et al., 2012; Chelamallu et al., 2013; Dietz et al., 2013), including validation with higher-resolution
159 [snow maps derived from satellite](#) imagery, such as from Landsat Thematic Mapper, Enhanced Thematic Mapper
160 Plus and Operational Land Imager (TM/ETM+ and OLI) (e.g., see Huang et al., 2011; Crawford, 2015; Coll and Li,
161 2018). [Crawford \(2015\) found strong spatial and temporal agreement between Terra MODIS snow-cover fraction](#)
162 [and Landsat TM/ETM+ derived snow cover, noting that some high-altitude cirrus cloud contamination was](#)
163 [observed and transient snow was sometimes difficult for the MODIS algorithm to detect.](#) Though use of higher-
164 resolution data is valuable [for comparison and validation purposes, however,](#) use of meteorological-station data [for](#)
165 [validation](#) (e.g., Brubaker et al., 2005) is the only true validation of [the](#) snow-cover products [when adequate station](#)
166 [data are available.](#) Comparing extent of snow cover derived from MODIS with snow cover from other satellite
167 products, [though extremely useful,](#) is not true validation because all derived snow-cover products have uncertainties.
168

169 A new feature of the MODIS C6 [and C6.1](#)-product suites provides the snow decision on each map as a normalized-
170 difference snow index (NDSI) value instead of fractional-snow cover (FSC) (Riggs et al., 2017a and 2018). This has
171 the important advantage of allowing a user to more-accurately determine FSC in their particular study area by
172 applying an algorithm [to derive FSC from the NDSI that is tuned they can tune to a specific study area to derive FSC](#)
173 [from the NDSI.](#) The C5 FSC algorithms (Salomonson and Appel, 2004 [& and 2006](#)) [is still useful for estimating](#)
174 [FSC globally for Terra MODIS data products, but is of more limited utility for specific and especially well-](#)
175 [characterized study areas. That algorithm remains useful globally](#) and can easily be applied to the MODIS C6 and
176 C6.1 and VIIRS [C1 and C2](#) NDSI data [to derive an estimate of FSC globally.](#)

177 178 **2.2- S-NPP VIIRS**

179
180 [There are 22 channels on the S-NPP VIIRS instrument. Though the the key VIIRS snow-mapping channels, I1](#)
181 [\(0.600 – 0.680 μm\) and I3 \(1.580 - 1.640 μm\), are also available on both VIIRS and MODIS \(with slight](#)
182 [differences in the wavelength range\), some of bands that are used in cloud mapping that are available on the MODIS](#)
183 [sensors, are not available on the VIIRS. As a result there are differences in the MODIS and VIIRS cloud masks that](#)
184 [affect the SCE standard products. Additionally, the Terra MODIS and the S-NPP VIIRS data are acquired at](#)
185 [different times of the day allowing for movement of clouds and for some snow-cover changes. Furthermore, the](#)
186 [spatial resolution of the MODIS SCE products is 500 m while the resolution of the VIIRS SCE products is 375 m.](#)
187

188 S-NPP VIIRS C2+ SCE products [<https://doi.org/10.5067/VIIRS/VNP10.001>] are designed to correspond to the
189 MODIS C6.1 SCE products (Riggs et al., 2017a and b). There were many revisions made in the MODIS C6 [and](#)

Formatted: Font color: Auto
Formatted: Font color: Auto

190 ~~C6.1~~ algorithms that improved snow-cover detection accuracy and ~~information content~~ QA of the data products.
191 Though there are important differences between the MODIS and VIIRS instruments (~~e.g., the VIIRS 375 m native~~
192 ~~resolution compared to MODIS 500 m~~), ~~some of which are described in the previous paragraph~~, the snow-detection
193 algorithms ~~and data products are~~ re designed to be as similar as possible so that the 19+ year MODIS ESDR of
194 global SCE can be extended into the future with the S-NPP and Joint Polar Satellite System (JPSS)-1 VIIRS snow
195 products and with products from future JPSS platforms.

197 ~~2.3.1~~ **Methods to reduce or eliminate cloud cover in MODIS-derived snow-cover maps**

198
199 ▲
200
201 The objective of the NASA standard MODIS and VIIRS CGF snow-cover algorithms is to generate snow maps
202 daily in the normal operational processing stream of MODIS and VIIRS snow products. As part of the early
203 MODIS snow-product suite, eight-day maximum snow-cover maps (M*D10A2) were designed to provide greatly-
204 reduced cloud cover. However these maps are available only once every eight days, the maps frequently retain
205 some cloud cover, and it is difficult to determine on which days during the eight-day period snow was or was not
206 observed; furthermore, only maximum observed snow cover is provided for any given eight-day period. In spite of
207 the limitations, the eight-day maximum snow maps have been useful in many studies (e.g., O’Leary et al., 2018;
208 Hammond et al., 2018). However, ~~the current~~ cloud-gap filling cloud-clearing method that uses current day and/or
209 previous day(s) of MODIS daily snow-cover products to fill gaps created by cloud cover ~~and is far superior to the~~
210 eight-day maximum method of cloud clearing.

211
212 Many effective methods have been developed to reduce or eliminate cloud cover in the MODIS standard snow-
213 cover products as well as other satellite-derived snow-cover products. These methods, including temporal and
214 spatial filtering, and use of data from two or more ~~than one~~ satellites. Fusion of ground and satellite measurements
215 is another method to mitigate the influence of clouds. ~~Though we cannot provide an exhaustive review here, in the~~
216 following paragraphs we refer to some of the methods. In the following paragraphs we provide a brief overview of
217 selected works that address the cloud-clearing issue using MODIS SCE products. ~~provide examples of cloud-cover~~
218 mitigation of snow cover maps standard. Our objective is to generate the CGF snow maps daily in the normal
219 operational processing stream of MODIS and VIIRS snow products. The cloud-clearing method uses current day
220 and/or recent previous day(s) of MODIS daily snow cover products to fill gaps created by cloud cover. ~~If timeliness~~
221 were not a constraint then interpolation of snow cover over time, both on previous and future days, could be a part of
222 a cloud clearing algorithm, and would increase the accuracy of the snow cover map on any given day.

Formatted: Font color: Red

226 The presence of cloud cover prevents daily continuous SCE maps from being produced using VNIR and SWIR
227 sensors. To reduce the effects of cloud cover in the MODIS snow cover maps, researchers have employed a variety
228 of different methods. As part of the early MODIS snow product suite, eight day maximum snow cover maps
229 (M²D10A2) were designed to provide greatly reduced cloud cover. However these maps are available only once
230 every eight days, the maps frequently retain some cloud cover, and it is difficult to determine on which days during
231 the eight day period snow was or was not observed. In spite of this, the eight day maximum snow maps have been
232 useful in many studies, e.g., M²D10A2 has been used successfully to develop snowmelt timing maps (O'Leary et
233 al., 2018) and to map snow zones (Hammond et al., 2018).

234 **and spatial.**

Formatted: Font: Bold

235

236 **Forward.**

Formatted: Font: Bold

237

238 Use of two or more days to map snow cover can be called temporal filtering. The presence of cloud cover prevents
239 daily continuous SCE maps from being produced using VNIR and SWIR sensors. To reduce the effects of cloud
240 cover in the MODIS snow cover maps, many researchers have employed a variety of different methods. For
241 example, as part of the early MODIS snow product suite, eight day maximum snow cover maps (M²D10A2) were
242 designed to provide greatly reduced cloud cover. However these maps are available only once every eight days, the
243 maps frequently retain some cloud cover, and it is difficult to determine on which days during the eight day period
244 snow was or was not observed. In spite of this, the eight day maximum snow maps have been useful in numerous
245 research studies, e.g., M²D10A2 has been used successfully to develop snowmelt timing maps (O'Leary et al.,
246 2018) and to map snow zones (Hammond et al., 2018), and are still available in C6.0 and 6.1.

Formatted: Font color: Red

247

248 Many other methods have also been developed to reduce or eliminate cloud cover in the MODIS snow cover
249 product suite. Parajka and Blöschl (2008) used a 7-day temporal filter causing a reduction of cloud coverage of
250 >95%, maintaining an overall accuracy of >92% when SCE was compared with in-situ data. Other methods to
251 reduce cloud cover have also been successful (e.g., see for example, Tong et al., 2009a & b; Coll and Li, 2018).
252 Gafurov and Bárdossy (2009) developed a cloud clearing method consisting of six sequential steps that begins with
253 using Terra and Aqua snow cover maps, ground observations, spatial analysis and finally snow climatology to clear
254 clouds and generate a cloud free daily snow cover map with high accuracy. Gafurov et al. (2016) developed an
255 operational daily snow cover monitoring tool using that same cloud clearing method with enhancements, with a
256 mean accuracy of 94% for a case study of the Karadarya River basin in Central Asia. To fill gaps caused by cloud
257 cover, use of forward and backward gap filling methods to eliminate cloud cover have been used successfully with
258 the MODIS standard snow products and other satellite data. Use of forward (e.g., Parajka and Blöschl, 2008;
259 Gafurov et al., 2016) and backward (e.g., Foppa and Seiz (2012)) and multi-temporal forward/backward
260 interpolation gap-filling methods to reduce cloud cover have been used successfully by many researchers with the
261 MODIS standard snow products and other satellite data (for example, see Parajka and Blöschl, 2008; Gafurov et al.,
262 2016; Malnes et al., 2016).

Formatted: Font color: Auto

263
264 Foppa and Seiz (2012) developed a temporal forward and backward gap fill method to create a “cloud-free” daily
265 snow map from the daily global MOD10C1 data product. Additionally, a Malnes et al. (2016) used a multi-temporal
266 forward/backward interpolation gap filling technique was used to create a cloud-free daily snow map from
267 MOD10A1 products that was then used to detect the first and last snow-free day in a season for northern Norway
268 (Malnes et al., 2016).

269 2.3.2 Spatial filtering

270
271
272 A spatial-filtering method that uses the relative position of a cloud-obscured pixel to the regional snow-line
273 elevation (SNOWL) was developed by Parajka et al. (2010) using Terra MODIS data to create “cloud-free” snow
274 maps which that produced robust snow-cover maps even in situations of extensive cloud cover.

Formatted: Not Highlight

Formatted: Not Highlight

Formatted: Not Highlight

275
276 A combination of SNOWL and temporal forward and backward gap filling was used by Hüsler et al. (2014) to
277 create “cloud-free” satellite snow-cover maps using data from the Advanced Very High Resolution Radiometer
278 (AVHRR) of the European Alps. Malnes et al. (2016) used a multi-temporal forward/backward interpolation gap-
279 filling technique to create a cloud-free daily snow map from MOD10A1 products that was then used to detect the
280 first and last snow-free day in a season for northern Norway. Gafurov and Bárdossy (2009) developed a cloud-
281 clearing method consisting of six sequential steps that begins with using Terra and Aqua snow cover maps, ground
282 observations, spatial analysis and finally snow climatology to clear clouds and generate a cloud-free daily snow-
283 cover map with high accuracy. 2Data-fusion methods of cloud clearing

284
285 A cubic spline interpolation method has been used with good results by some researchers (Tang et al., 2013 & 2017;
286 Xu et al., 2017) as a temporal CGF method using MODIS snow cover products. Some researchers have developed
287 CGF techniques that combined Terra and Aqua, time interpolation, spatial interpolation and probability estimation,
288 e.g. López-Burgos et al. (2013) to create “cloud-free” SCA maps. Deng et al. (2015) combined MOD, MYD and
289 SNOWL, SCE and AMSR2 SWE data and temporal filtering to create a daily “cloud-free” snow cover maps of
290 China. Combining different methods sequentially to remove clouds is also a way to create CGF products (Darlane
291 et al., 2017). A cubic spline interpolation method has been used with good results by some researchers (Tang et al.,
292 2013 & 2017; Xu et al., 2017) as a temporal CGF method using MODIS snow cover products. Crowdsourcing by
293 cross-country skiers combined with MODIS snow cover products has also been used to create daily CGF products
294 (Kadlec and Ames, 2017).

295
296 A common method to reduce cloud cover on a daily snow map is to combine or fuse results from the daily Terra
297 (MOD10A1) and Aqua (MYD10A1) snow maps (see for example, Gao et al., 2010a & 2010b and 2011+;
298 Li et al., 2017; Paudel and Anderson, 2011; Thompson et al., 2015; Dong and Menzel, 2016; Yu et al., 2016; Xu et
299 al., 2017). Dong and Menzel (2016) developed a multistep method including probability interpolation, to eliminate

cloud-cover using combined Terra-Aqua MODIS snow-cover products. These methods take advantage of the fact that the Terra and Aqua satellite overpasses occur at different times of the day and, since clouds move, oftentimes more snow cover or non-snow-covered land cover can be imaged and mapped using data from both satellites, as compared to using the Terra or Aqua MODIS data alone. However, Though this method of cloud clearing is useful, it is of limited utility for large areas because changes in cloud cover are typically small between Terra's 10:30 am local time equator crossing and Aqua's at 1:30 pm.

Additionally, Percent reductions in cloud cover that are achieved by combining Terra and Aqua daily snow-cover data are highly variable and dependent on many factors such as location, time of year, daily weather and cloud conditions, etc., and have been reported to vary. A factor that impacts the quality of both the Aqua MODIS snow-cover and the cloud-cover products, used to mask clouds, is that many of the detectors in the critical 1.6 μm band used in both algorithms is non-functional on the Aqua MODIS. As an example, for the western U.S. study area shown in Fig. 1, for 14 March 2012 and 19 March 2012, using a snow-cover map that combined Terra and Aqua snow cover products, the MOD10A1 snow product showed 71.7 percent clouds while the combined Terra and Aqua products showed 67.0 percent for 14 March 2012. For another date, 19 March 2012, MOD10 showed 71.8 percent clouds while the combined Terra/Aqua snow map showed 68.4 percent. Combining the MOD and MYD snow maps definitely can reduce cloud cover but there are issues with the Aqua snow maps (see below) and reliance on the continued availability of two nearly-identical sensors is problematic unrealistic for development of an ESDR because satellites do not last indefinitely.

Formatted: Strikethrough, Highlight

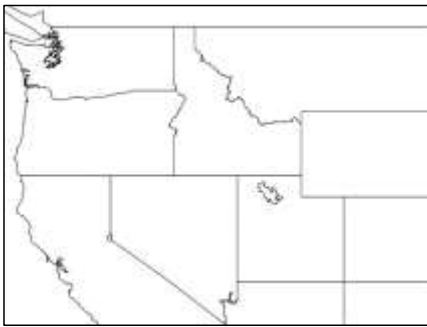
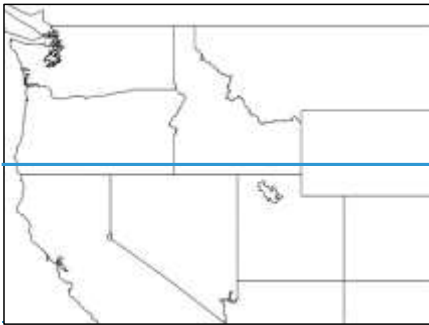


Figure 1: Study area covering all or parts of 11 states in the western United States and part of southern Canada. This study area is 2,487,610 km² in area.

2.3.4 Fusion of ground and satellite measurements



327
328 **Figure 1:** Study area covering all or parts of nine states in the western United States and part of southern Canada. The following
329 MODIS tiles were used to develop the composite: h08v04, h09v04, h10v04, h08v05, h09v05, h10v05.

330 Fusion of ground-based and satellite-based snow observations is also an effective approach to map snow-cover“see
331 beneath” clouds. This method of cloud clearing is used successfully by NOAA to develop the Interactive
332 Multisensor Snow and Ice Mapping System (IMS) SCE products (see Helfrich et al., 2007 and 2012).
333

334
335 Hybrid methods to reduce cloud cover are also effective. For example, Gafurov and Bárdossy (2009) developed a
336 cloud-clearing method consisting of six sequential steps that begins with using Terra and Aqua snow cover maps,
337 ground observations, spatial analysis and finally snow climatology to clear clouds and generate a cloud-free daily
338 snow-cover map with high accuracy. Other researchers have developed CGF techniques that combined Terra and
339 Aqua, time interpolation, spatial interpolation and probability estimation, e.g. López-Burgos et al. (2013) to create
340 “cloud-free” SCEA maps. Deng et al. (2015) combined MOD, MYD and SNOWL SCE and AMSR2 SWE data and
341 temporal filtering to create daily “cloud-free” snow cover maps of China. Combining different methods sequentially
342 to remove clouds is also a way to create CGF products (Dariane et al., 2017). A cubic spline interpolation method
343 has been used with good results by some researchers (Tang et al., 2013 & 2017; Xu et al., 2017) as a temporal CGF
344 method using MODIS snow cover products. Crowdsourcing by cross-country skiers combined with MODIS snow-
345 cover products has also been used to create daily CGF products (Kadlec and Ames, 2017). Many other methods to
346 reduce cloud cover have also been successful (e.g., see for example, Tong et al., 2009a & b; Tang et al., 2013 &
347 2017; Xu et al., 2017; Dariane et al., 2017; Xu et al., 2017; Coll and Li, 2018).
348

349 The CGF method of Hall et al. (2010) and Riggs et al. (2018) is the method that was selected for the NASA MODIS
350 standard SCE products because of its ease-of-use, effectiveness and because it relies on data from only one sensor at
351 a time to produce results.
352

353 **2.4 Differences between Terra and Aqua MODIS snow-cover maps**

Formatted: Font: Not Bold

Formatted: Font: Bold

354
355 ~~Beginning in~~Since the MODIS C6 re-processing, the Quantitative Image Restoration (QIR) algorithm (Gladkova et
356 al., 2012) has been used in the Aqua MODIS snow algorithm to restore ~~the~~lost data from ~~the~~non-functional band 6
357 detectors so that the same snow-cover mapping algorithm can be used in both Terra and Aqua. ~~Beginning with the~~
358 ~~launch of the Aqua MODIS, some detectors in Aqua MODIS band 6 have not functioned~~Since band 6 (with a
359 center wavelength of ~1.6 μm) is, a key band for ~~to~~ snow-cover SCE mapping, experienced degradation issues even
360 before the launch of the Aqua satellite in 2002 and many of its detectors are non-functioning ~~there was a degradation~~
361 ~~in the Aqua MODIS SCE mapping algorithm as compared to the Terra MODIS algorithm~~. Therefore, ~~for C5 and~~
362 ~~earlier collections, Aqua MODIS band 7 (~2.1 μm) was used instead of band 6 in the snow-mapping algorithm~~
363 (Riggs et al., 2006). ~~Additionally, An additional complication is that t~~The cloud-masking algorithm for Terra uses
364 MODIS band 6 but the cloud-masking algorithm for ~~the~~ Aqua algorithm was adapted to use band 7 instead of band
365 6 ~~because of the non-functioning detectors in Aqua band 6 for Collection 5 and earlier collections~~. This resulted in
366 the Terra and Aqua algorithms often providing different snow-mapping results ~~in many snow-covered areas due to~~
367 ~~the reduced accuracy of the Aqua algorithm~~. ~~I~~However, even in C6 and C6.1 in which the QIR is employed ~~to map~~
368 ~~snow in both the Terra and Aqua SCE algorithms~~, there are still more cloud/snow discrimination errors in the Aqua
369 cloud-mask algorithm as compared to the Terra algorithm ~~because the QIR is not used for cloud masking within the~~
370 ~~Aqua datacloud mask~~. This results in more snow commission errors in MYD10L2 (Aqua) ~~snow maps~~ as compared
371 to MOD10L2 (Terra) ~~snow maps~~. ~~Because of the greater uncertainties inherent in snow mapping using MYD10~~
372 ~~algorithms for reasons mentioned above, and because any combined method using both Terra and Aqua data is~~
373 ~~dependent on more than one sensor providing data, we do not recommend the Aqua MODIS SCE product to be part~~
374 ~~of a planned MODIS VIIRS ESDR for SCE~~. ~~Additionally, since both the Terra and Aqua MODIS sensors are well~~
375 ~~beyond their design lifetimes, it is not realistic to depend on both to provide data indefinitely into the future.~~

376
377 Fusion of ground-based and satellite-based snow observations is also an effective approach to “see beneath” clouds.
378 This method of cloud clearing is used by NOAA to develop the Interactive Multisensor Snow and Ice Mapping
379 System (IMS) SCE products (see Helfrich et al., 2007 and 2012).

380
381 Our objective is to generate the CGF snow maps daily in the normal operational processing stream of MODIS and
382 VIIRS snow products. The cloud clearing method uses current day and/or recent previous day(s) of MODIS daily
383 snow cover products to fill gaps created by cloud cover. If timeliness were not a constraint then interpolation of
384 snow cover over time, both on previous and future days, could be a part of a cloud clearing algorithm, and would
385 increase the accuracy of the snow cover map on any given day.

386 387 **3 Methodology and Results**

388
389 ~~The new standard CGF products of Collection 6.1 and C2, respectively, M*~~D10A1F~~ and VNP10A1F, enable~~
390 ~~researchers to download and use cloud-free MODIS and VIIRS daily snow SCE maps along with quality assurance~~

Formatted: Font color: Auto

Formatted: Strikethrough

391 (QA) data information to assess uncertainties of the gap-filling algorithm. Reference Figure 1 here. Study Here For
392 the present work, we focus on a large (2,487,610 km²) study area covering all or parts of 11 states in the western
393 U.S. and part of southern Canada (Figure 1). Examples of the daily Terra MODIS standard and CGF and the daily
394 S-NPP VIIRS standard and CGF cloud-free map products for this western U.S. study area (Fig. 1) may be seen
395 in Fig. 2. Note some differences in cloud cover between the Terra MODIS (top left) and S-NPP
396 VIIRS (top right) standard snow maps. The MOD10A1F scene snow map is 65.8 percent (1,637,066 km²) cloud-
397 covered, vs 60.6 percent (1,506,924 km²) in the VNP10A1F snow map. The difference in cloud coverage is largely
398 due to the differences in the cloud masking of MODIS and VIIRS SCE maps, as described earlier. However,
399 difference in the locations of clouds is also a contributing factor because the Terra MODIS and S-NPP VIIRS
400 images were acquired at different times on the same day, and clouds move. There may also be changes in the
401 location of snow cover within a day (due to melting of shallow snow, for example). Even given these small
402 differences in the standard products that include clouds, the CGF snow maps shown in the bottom row of Fig. 2 are
403 very similar, with 15.2 percent (378,634 km²) snow cover on the MOD10A1F snow map and 16.6 percent (413,794
404 km²) snow cover on the VNP10A1F snow map. Thus the VIIRS maps shows fewer clouds and more snow than
405 does the Terra MODIS map in this example.

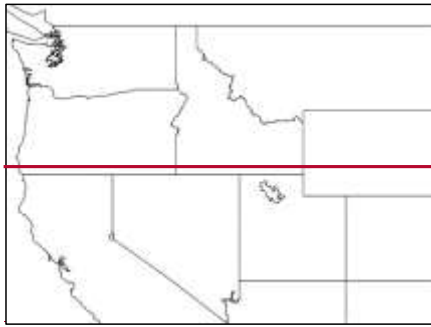
406
407 in area. Examples of the dThe daily Terra MODIS CGF S-NPP SCE product is similar to MOD10A1 product but is
408 cloud-free for the western U.S. study area (Fig. 1), as seen in Fig. 2. There are some differences in cloud cover
409 between the Terra MODIS (top left) and S-NPP VIIRS (top right) snow maps. The percentage of clouds in the
410 MOD10A1F scene is 65.8 percent (1,637,066 km²), vs 60.6 percent (1,506,924 km²) in the VNP10A1F snow map.
411 The difference in cloud coverage is largely due to the differences in the cloud masking of MODIS and VIIRS,
412 described earlier. It is However there also a factor because the images were acquired at different times on the same
413 day, and clouds move. Perhaps even some changes in snow cover. The CGF snow maps shown in the bottom row
414 of Fig. 2 are very similar, with 15.2 percent (378,634 km²) snow cover on the MOD10A1F snow map and 16.6
415 percent (413,794 km²) snow cover on the VNP10A1F snow map, with VIIRS modis/viirs mapping more snow than
416 MODIS.

417
418 the accuracy of the snow observation depends in part on the age of the observation, i.e., number of days since last
419 cloud-free observation, thus information on cloud persistence is included with each product. The accuracy of the
420 observation at the pixel-level depends on the cloud masking of the swath product, M[#]D10-L2, for MODIS and
421 VNP10-L2 for VIIRS. The MODIS and VIIRS snow cover swath products are gridded and mapped into the daily
422 tiled products that are input to M[#]D10A1F and VNP10A1F CGF algorithms.

423

- Formatted: Font color: Auto
- Formatted: Font: (Default) Times New Roman, 10 pt
- Formatted: Font color: Auto
- Formatted: Font color: Auto
- Formatted: Font: (Default) Times New Roman, 10 pt
- Formatted: Font: (Default) Times New Roman, 10 pt
- Formatted: Font: (Default) Times New Roman, 10 pt
- Formatted: Font color: Auto
- Formatted: Font color: Auto
- Formatted: Font: (Default) Times New Roman, 10 pt
- Formatted: Superscript
- Formatted: Superscript

- Formatted: Font color: Auto
- Formatted: Font color: Auto
- Formatted: Font: (Default) Times New Roman, 10 pt
- Formatted: Font color: Auto
- Formatted: Font: (Default) Times New Roman, 10 pt
- Formatted: Font color: Auto
- Formatted: Font color: Auto
- Formatted: Font color: Auto
- Formatted: Font: (Default) Times New Roman, 10 pt
- Formatted: Font color: Auto
- Formatted: Font: (Default) Times New Roman, 10 pt
- Formatted: Font color: Auto
- Formatted: Font color: Auto
- Formatted: Highlight
- Formatted: Font color: Auto
- Formatted: Font color: Auto



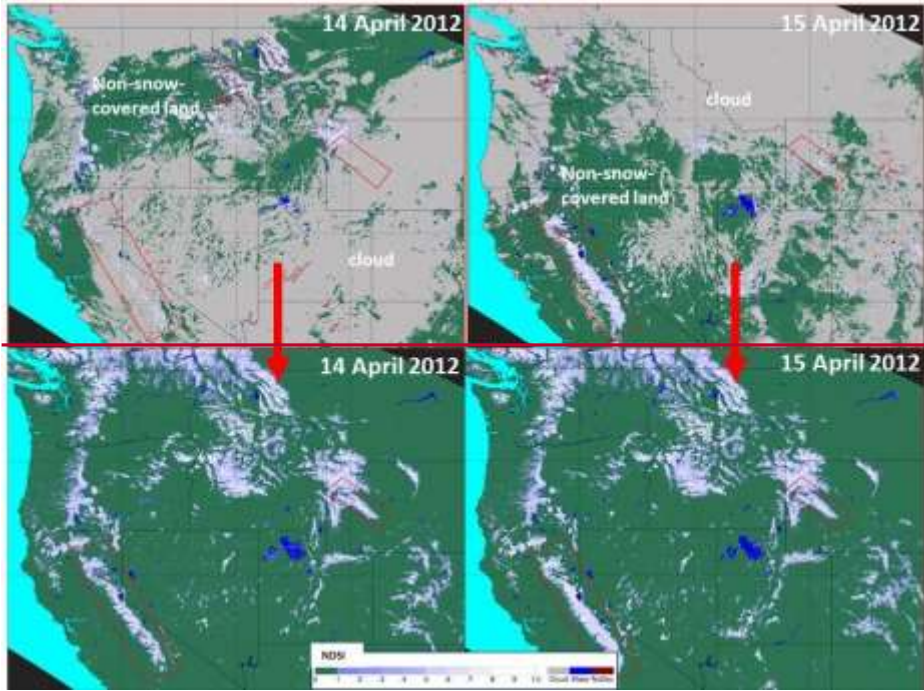
424

425 **Figure 1:** Study area covering all or parts of nine states in the western United States and part of southern Canada. The following
426 MODIS files were used to develop the composite: h08v01, h09v01, h10v01, h08v05, h09v05, h10v05. The areal extent of this
427 study area is 2,487,610 km².

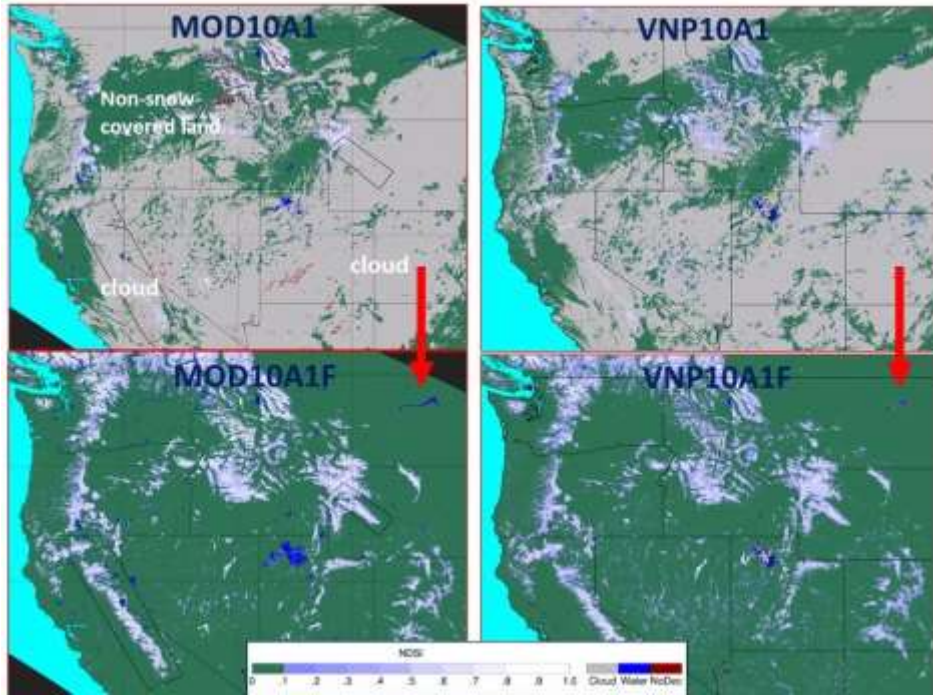
428

429

430



431



432
433
434 **Figure 2: Top Row**—Examples of the C6 MOD10A1 and the new Collection 6.1 MOD10A1F MODIS snow maps and
435 VIIRS standard and cloud-gap filled (CGF) snow maps on 14 April 2012 for a study area in the western United
436 States/southwestern Canada (see Fig. 1). **Top row left:** MODIS MOD10A1 C6.1 snow maps showing extensive cloud cover on
437 14 and 15 April 2012. **Top right:** VIIRS VNP10A1 C1 snow map also showing extensive cloud cover on 14 April 2012.
438 **Bottom left row:** MOD10A1F C6.1 cloud-gap filled (CGF) maps corresponding to the MOD10A1 snow maps in the top row,
439 also for 14 and 15 April 2012. **Bottom right:** VNP10A1F CGF map corresponding to the VNP10A1 snow map in the top row,
440 also for 14 April 2012. In all of the snow maps, Non-snow-covered land is green. Regions of interest (ROI) containing the
441 Sierra Nevada Mountains in California and Nevada (109,575 km²), and the Wind River Range in Wyoming (22,171 km²), are
442 outlined in red on the MODIS snow maps. The following MODIS tiles were used to develop the MODIS composites: h08v04,
443 h09v04, h10v04, h08v05, h09v05, h10v05. Each VIIRS swath that included coverage of this study area was composited to create
444 a daily map, then the daily maps were used to create the VNP10A1F snow map for 14 April 2012.

445
446
447 **REVISE this FIGURE. Instead of showing the 15 April 2012 MODIS image pair, replace that with 14 April VIIRS snow**
448 **maps.**

Formatted: Font color: Auto

Formatted: Font: (Default) Times New Roman, 9 pt

Formatted: Font: (Default) Times New Roman

Formatted: Font: (Default) Times New Roman

Formatted: Font: (Default) Times New Roman

Formatted: Font: (Default) Times New Roman, 9 pt

Formatted: Font: Bold

Formatted: Font color: Red

Formatted: Font: 9 pt

450 Though cloud gap filling provides a cloud free snow map every day, the accuracy of the snow observation depends
451 in part on the age of the observation, i.e., number of days since last cloud free observation, thus information on
452 cloud persistence is included with each product. The accuracy of the observation at the pixel level depends on the
453 snow cover algorithm that includes cloud masking of the swath product, M*D10_L2, for MODIS and VNP10_L2
454 for VIIRS. The MODIS and VIIRS snow cover swath products are gridded and mapped into the daily tiled products
455 which that are input to M*D10A1F and VNP10A1F CGF algorithms.

456
457 The accuracy of the snow observation is dependent on many factors. In this work, we focus on the uncertainties of
458 the gap-filling method; we do not address the inherent accuracy of the snow maps because that has been
459 documented elsewhere by many previous studies, at least for the MODIS SCE products. The accuracy
460 of Uncertainties in the CGF maps that relate to the gap-filling methodology, shown in Fig. 2 depends in part on the
461 age of the observation, i.e., number of days since last cloud-free observation. To address this, information on cloud
462 persistence for each pixel is included with each product. The accuracy of the observation at the pixel level also
463 depends on the Cloud masking of the swath product, M*D10_L2, for MODIS and VNP10_L2 for VIIRS,
464 represents an additional uncertainty in the both products and contributes to differences between the snow-mapping
465 results. The MODIS and VIIRS snow-cover swath products are gridded and mapped into the daily tiled products
466 that are input to M*D10A1F and VNP10A1F CGF algorithms (Riggs et al., 2017a).

467
468 For MODIS, inputs to the MODIS CGF algorithms are the current day M*D10A1 and the previous day
469 M*D10A1F products. The CGF daily snow map is created by replacing cloud observations in the current day
470 M*D10A1 with the most-recent previous cloud-free observation from the M*D10A1F (Hall et al., 2010; Riggs et
471 al., 2018). The algorithm tracks the number of days since the last cloud-free observation by incrementing the count
472 of consecutive days of cloud cover for a pixel. This is stored in the cloud-persistence count (CPC) data array. If the
473 current day observation is 'cloud' then the cloud count is one and is added to the CPC count from the previous day's
474 M*D10A1F and written to the current day's M*D10A1F algorithm. If the current day observation is 'not cloud,'
475 then the CPC is reset to zero in the current day's M*D10A1F CPC. If the CPC is 0, that means that the snow-cover
476 observation is from the current day. If the CPC for the current day is ≥ 1 , that represents the count of days since the
477 last 'non-cloud' observation. On the day that the CGF mapping algorithm is initialized for a time series, for
478 example, 1 xx February 2012, the CGF snow-cover map is identical to the MODIS daily snow-cover map
479 (M*D10A1) and the cloud-persistence count (CPC) map will show zeros for non-cloud observations and ones for
480 cloud observations (Riggs et al., 2018). As the time series progresses, a nearly-cloud-free snow map is produced on
481 about Day 5-8 in theis example, shown in Fig. 3, on whichwhen the percent clouds cover is only 3.88.0 percent of the
482 snow map (Fig. 3), though it takes 24 days to achieve a completely cloud free map in this example (not shown).
483 The same method is used to develop the VNP10A1F CGF snow-map products. For the same initialization of the
484 time series, beginning on 4 February 2012, a nearly-cloud-free snow map is produced on Day 5x when the clouds
485 cover is only xxx6.7 percent of the map, and it takes xxx days to achieve a completely cloud free VNP10A1F CGF
486 snow map (Fig. 3).

Formatted: Font color: Auto

Formatted: Font color: Auto

Formatted: Font color: Auto

Formatted: Font color: Auto

Formatted: Font color: Auto

Formatted: Font color: Auto

Formatted: Font color: Auto

Formatted: Font color: Auto

~~PCT_CLOUD_MODIS_CGF_ALL~~

~~61.23 36.52 25.18 19.19 15.94 11.20 10.16 8.03 5.74 4.16~~

~~PCT_CLOUD_VIIRS_CGF_ALL~~

~~50.78 23.28 14.21 10.20 6.71 4.70 4.48 3.18 2.17 2.02~~

Formatted: Strikethrough, Highlight

Formatted: Strikethrough

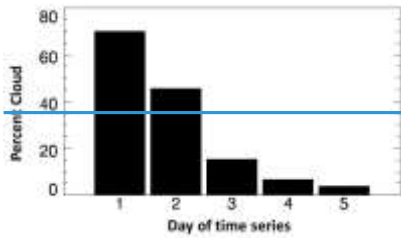


Figure 3: Percent cloud cover on a scene from the western United States (see location of the study area in Fig. 1). Note that the percentage of cloud cover decreases dramatically in the first few days following the beginning initiation of the CGF time series on 4 February 2012, herein denoted as Day 1. The percent cloud cover drops from about 75 percent on Day 1 to 3.8

Formatted: Font color: Red

Formatted: Font color: Red

Formatted: Font color: Red

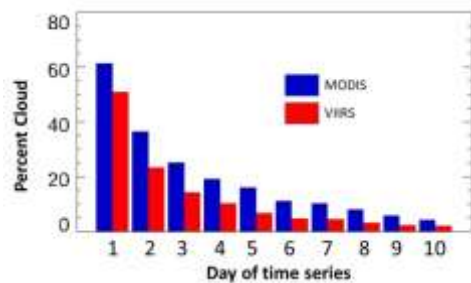


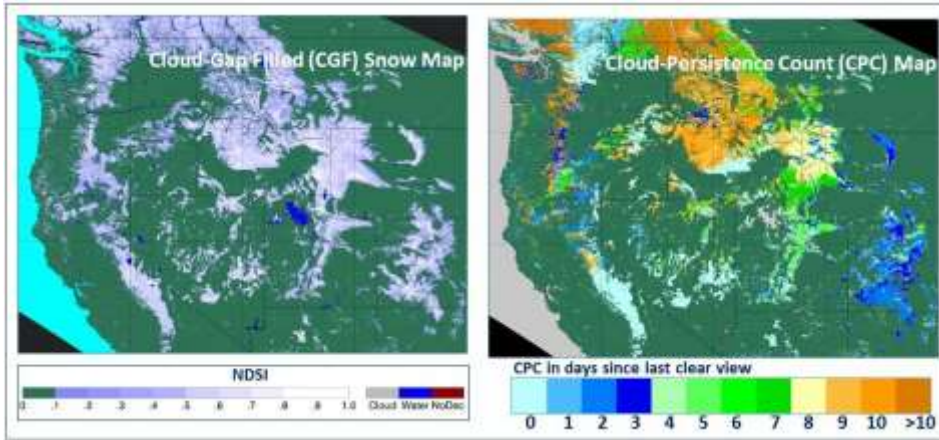
Figure 3: Percent cloud cover in a Terra MODIS (MOD10A1F) and an S-NPP VIIRS (VNP10A1F) time series of snow-cover maps for the western United States study area (see location in Fig. 1). Note that the percentage of cloud cover decreases dramatically in the first few days following the 4 February 2012 initiation of the CGF time series, denoted here as Day 1. In this example, the percent cloud cover drops from about xx percent on Day 1 to xx percent on Day 5 for the MOD10A1F time series and xx percent on Day 1 to xxx percent on Day x for the VNP10A1F time series.

Formatted: Font color: Red

Formatted: Font: Not Bold

A CPC data arraymap is associated with each CGF snow map so that a user may determine the age of the snow observation of each pixel (Fig. 4). For each pixel, the uncertainty of the observation increases with time since the last clear view. To help a user assess the accuracy of an observation, the count of consecutive days of cloud cover is incremented and stored as QA in the CPC map that specifies how far back in time the observation was acquired. For example, for 19 March 2012, when a pixel has a CPC = 0, this means that the reported NDSI value for that pixel was acquired on 19 March 2012. When a pixel has a CPC=1 this means that the reported NDSI pixel value is one day old, hence it was acquired on 18 March, and so on (Fig. 4). A user can decide how far back in time they would like

511 to use an observation, and can easily develop a unique CGF map, utilizing the CPC information that is most
 512 appropriate for their application.
 513
 514



515
 516
 517 **Figure 4:** Left -- Terra MODIS cloud-gap filled (CGF) MOD10A1F snow map for 19 March 2012. Right -- Cloud-persistence
 518 count (CPC) map from the quality assurance (QA) dataset for the 19 March CGF snow map seen at left. For 19 March 2012,
 519 when a pixel has a CPC = 0, this means that the NDSI value for that pixel was acquired on 19 March 2012. When a pixel has a
 520 CPC=1 this means that the NDSI pixel value is one day old, hence it was acquired on 18 March, and so on.

521
 522 For the snow-cover product suite, the time series are started with the first day of acquisition for each mission, then
 523 reset when on October 1st is reached of each year. The first days of the gap-filling time series for the Terra and Aqua
 524 MODIS CGF production are 24 February 2000 and 24 June 2002, respectively. The first day of gap filling for the S-
 525 NPP VIIRS CGF production is the first day of VIIRS data collection which is 21 November 2011. With those
 526 exceptions, gap-filling sequences begin on the first day of each water year, October 1st.

527
 528 The MODIS data-acquisition record is nearly continuous from the beginning of the missions however, there are brief
 529 periods -- minutes to hours -- when either the Terra
 530 [https://modaps.modaps.eosdis.nasa.gov/services/production/outages_terra.html] or Aqua
 531 [https://modaps.modaps.eosdis.nasa.gov/services/production/outages_aqua.html] MODIS data were not acquired or
 532 data were "lost." In general, those outages have minimal effect on the snow-cover data record. There have also
 533 been some VIIRS data outages which are also tracked
 534 [https://modaps.modaps.eosdis.nasa.gov/services/production/outages_npp.html].
 535 However, in addition, there are also a few rare extended data outages of one to five days that have occurred in the
 536 MODIS Terra record. Extended outages, and may occur in the future. --George, do you know of gaps in the VIIRS

Formatted: Font: 9 pt

Formatted: Font: 9 pt

Formatted: Font: 10 pt

Formatted: Font: (Default) Times New Roman, 10 pt

Formatted: No Spacing, Line spacing: 1.5 lines

Formatted: Font: (Default) Times New Roman, 10 pt

Formatted: Font: (Default) Times New Roman, 10 pt

Formatted: Font: (Default) Times New Roman

537 [data record?](#) The gap-filling algorithms for both MODIS and VIIRS are designed to continue processing over daily
538 or multi-day gaps in the data record. A missing day of MODIS or VIIRS ~~NDSI~~ snow-cover input is processed as if
539 it were completely cloud obscured so the previous day's CGF result is retained and the CPC is incremented by one.
540 Orbit gaps and missing swath or scan line data within a tile are processed as a cloud observation with the previous
541 good observation retained and the CPC is incremented for the current day. This provides a continuous [snow-cover](#)
542 data record for the CGF product. See Riggs et al. (2018) for further details.

544 **4 Results: 3-1 Evaluation and Validation Analysis**

545
546 ~~In this section, we provide evaluation and validation for study areas in the western United States and a study area in~~
547 ~~the northeastern United States/southeastern Canada. We also look at regions of interest (ROIs) within the primary~~
548 ~~western United States study area shown in Figure 1. T~~At the time of this writing, the MODIS and VIIRS CGF SCE
549 ~~products are not yet~~will be available to download s. Sometime during the fall of 2019 the products will be
550 ~~downloadable through the National Snow and Ice Data Center (NSIDC) in Boulder, Colorado, USA. To enable~~
551 ~~some early evaluation of the products we produced CGF Terra and Aqua MODIS time series of selected areas in the~~
552 ~~western U.S. and in the northeastern U.S. and southeastern Canada. Here we provide evaluation and some~~
553 ~~validation for study areas in the western U.S./southwestern Canada and a study area in the northeastern~~
554 ~~U.S./southeastern Canada. We also look at regions of interest (ROI) within our~~the primary western
555 ~~U.S./southwestern Canada study area shown in Fig. 1. To begin to evaluate the products we produced Terra and~~
556 ~~Aqua MODIS time series of areas in the western U.S. and in the northeastern U.S. and southeastern Canada. We~~
557 ~~selected the year 2012 for the time series because both MODIS and VIIRS data were available in that year.~~
558 Comprehensive global validation studies will not be possible to perform until the data sets are released through
559 NSIDC and the entire MODIS and VIIRS records have been processed. This ~~may~~will take several months following
560 ~~initial release of the data; the full data records should be available in 2020.~~

561
562 There are many ways to evaluate the uncertainties in the CGF snow-cover maps but only one way to [perform](#)
563 [absolute validation](#) of the maps. The CGF maps can be compared with other daily snow-cover map products (e.g.,
564 NOAA IMS 4-km snow maps Helfrich et al., 2007 [and](#); 2012; Chen et al., 2012), with snow maps developed from
565 higher-resolution maps such as from Landsat and Sentinel₁, and with reflectance images derived from satellite data.
566 This allows ~~us to evaluate~~[evaluation of](#) the products but does not constitute [absolute](#) validation.

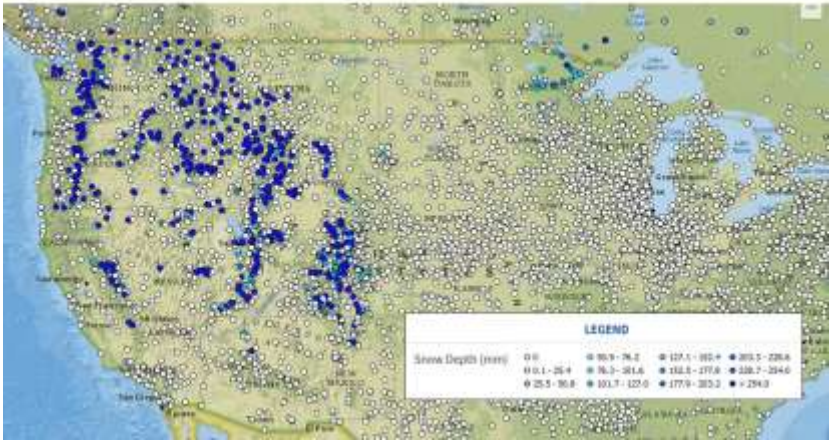
567
568 ~~In the U.S., the SCE~~The only way to validate the products ~~can be validated~~is using NOAA snow depth data
569 <https://gis.ncdc.noaa.gov/maps/ncei/summaries/daily> as has been done for MOD10A1 (Collections 1 – 5) by many
570 authors (e.g., Brubaker et al., 2005; Chen et al., 2012). However the density of meteorological stations is highly
571 variable ~~in the U.S. and the network of meteorological station data over the globe is even more variable, especially~~
572 ~~in higher latitudes. Therefore the snow maps can only truly be validated where there is a dense network of~~

573 meteorological stations, though we can sometimes successfully interpolate between stations when stations are
574 farther apart.
575

576 **4.1 Compare with Validation using NOAA snow depth data.**

577
578 Snow depths from NOAA snow depth data (e.g., see Fig. 5) can be overlain on a MODIS CGF snow map as shown
579 in the example in Figures 6 and 7. Based on NOAA snow-depth data indicating the presence of snow cover, on
580 16 April 2012 the Terra MODIS CGF map appears to map the location of snow cover very well in an ROI in Utah
581 that includes part of the Wasatch Range, based on NOAA snow depth data indicating the presence of snow cover. A
582 NASA WorldView true-color (corrected reflectance) Terra MODIS image is shown alongside a Terra MODIS CGF
583 snow map with NOAA snow depths superimposed on an ROI in south-central Utah (Fig. 6a, b & c). There are no
584 other NOAA stations that report snow cover except the ones shown in Fig. 6b. The dark blue and light blue circles
585 indicate snow depths of up to or ≥ 254.0 mm, and the white circle indicates a snow depth of 0.1 – 25.4 mm,
586 revealing that the MOD10A1F snow map accurately reflects shows the location of snow cover in this ROI.
587
588

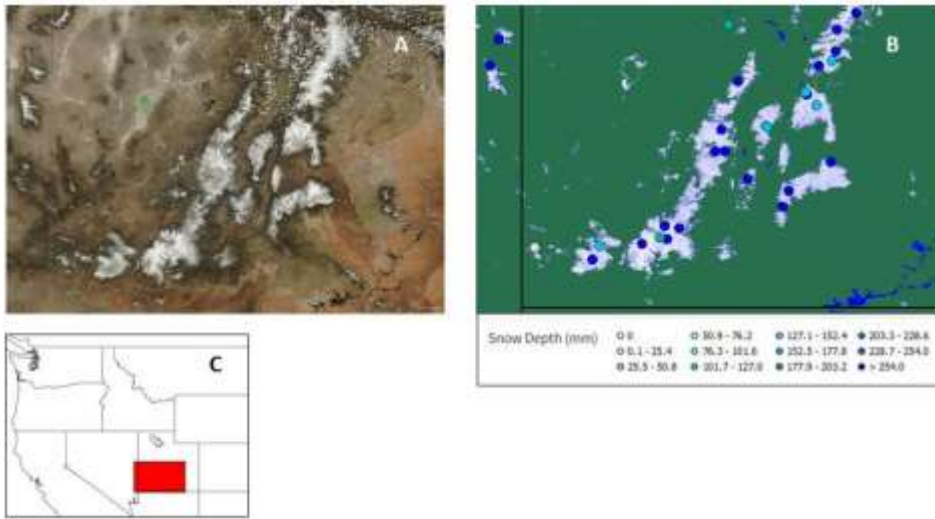
- Formatted: Font: Bold
- Formatted: Font: Bold, Not Italic, No underline
- Formatted: Font: Bold
- Formatted: Font: Bold, Not Italic, No underline



589
590 **Figure 5:** Snow depth (mm) from 16 April 2012 for part of the continental United States. Source: NOAA National Climate Data
591 Center <https://gis.ncdc.noaa.gov/maps/ncei/summaries/daily>.

592
593 On 16 April 2012 the MODIS CGF map appears to map the location of snow cover very well in an ROI in Utah that
594 includes part of the Wasatch Range, based on NOAA snow depth data indicating the presence of snow cover. A
595 NASA WorldView true color (corrected reflectance) Terra MODIS image is shown alongside a Terra MODIS CGF

596 snow map with NOAA snow depths superimposed on an ROI in south-central Utah (Fig. 6a, b & c). There are no
 597 other NOAA stations that report snow cover except the ones shown in Fig. 6b. The dark blue and light blue circles
 598 indicate snow depths of up to or >254.0 mm, and the white circle indicates a snow depth of 0.1–25.4 mm, revealing
 599 that the MOD10A1F snow map accurately reflects the location of snow cover in this ROI.
 600



601
 602 **Figure 6a:** NASA WorldView true-color (corrected reflectance) Terra MODIS image of a region on interest (ROI) in central
 603 Utah, USA-S-A, including the southern part of the Wasatch Range, acquired on 16 April 2012. Fig. 6b. Snow depths from
 604 NOAA are mapped onto the Terra MODIS CGF map, MOD10A1F, for 16 April 2012 for the same area shown in Fig. 6a. Open
 605 circles indicate stations that report snow depth, though none is visible in this snow map. Fig. 6c. Location map where the red
 606 rectangle delineates the ROI.

607 **3.114.2. Compare with higher-resolution images and derived snow maps.**

608
 609 In the absence of meteorological-station data or in addition to it, a good way to evaluate the accuracy of the
 610 MODIS CGF SCE maps is to compare them with snow maps derived from higher-resolution sensors such as from
 611 the Sentinel-2A (S-2A) Multispectral Instrument (MSI) 30-m resolution images derived from the Harmonized
 612 Landsat Sentinel-2 (HLS) dataset [https://hls.gsfc.nasa.gov/] (Claverie et al., 2018). As an example, we compare
 613 snow cover mapped in MODIS CGF snow cover products with snow cover derived from Sentinel 2A Multispectral
 614 Instrument (MSI) 30-m resolution images from the Harmonized Landsat Sentinel 2 (HLS) dataset
 615 [https://hls.gsfc.nasa.gov/] (Claverie et al., 2018) as seen in for an ROI in Montana, in (Fig. 7a and; b & show a
 616 comparison of an S-2A image and a Terra MODIS CGF snow map from 2 December 2016).

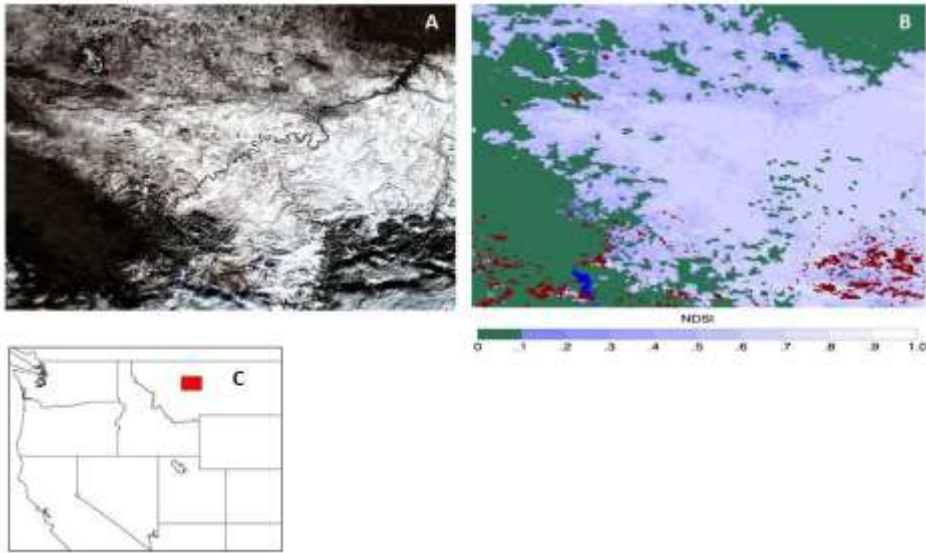
Formatted: Font: Bold, Not Italic, No underline

Formatted: Font: Bold

Formatted: Font: Bold, Not Italic, No underline

Formatted: Font: Bold

617
618
619



620
621 **Figure 7a:** Sentinel-2A 'true-color' image showing snow cover in shades of white and grey, acquired on 2 December 2016 for a
622 region of interest (ROI) in the state of Montana, U.S.A.. Black indicates non-snow-covered ground. Fig. 7b. The MOD10A1F
623 cloud-gap-filled (CGF) snow map of the same area and on the same date as is shown in Fig. 7a. In the CGF snow map in Fig. 7b,
624 snow is depicted in various shades of white and purple, corresponding to Normalized Difference Snow Index (NDSI) values.
625 Pixels shown in red represent 'no decision' by the NDSI algorithm. Fig. 7c. The red box corresponds to the location of the
626 images in the ROI in Montana, shown in Fig. 7a and Fig. 7b.
627

628 Snow cover on 2 December 2016 may be seen on the Sentinel-2A (S-2A) image in shades of white and grey from
629 this RGB composite image (bands 4, 3 and 2 (red (664.6 nm), green (559.8 nm) and blue (492.4 nm), respectively))
630 in Fig. 7a. Though the location of snow cover in the S-2A image is visually very close to the snow cover depicted
631 in shades of purple to white in the CGF snow map of Fig. 7b, there is not perfect correspondence. The point of this
632 comparison is to demonstrate the utility of high-resolution imagery to evaluate the CGF maps, not to perform a
633 detailed and quantitative comparison that would involve our selecting an algorithm to map snow cover in the S-
634 2AS2 image, with its inherent uncertainties. Therefore this is an example of evaluation and comparison of snow
635 maps, and not validation of the CGF map product.
636

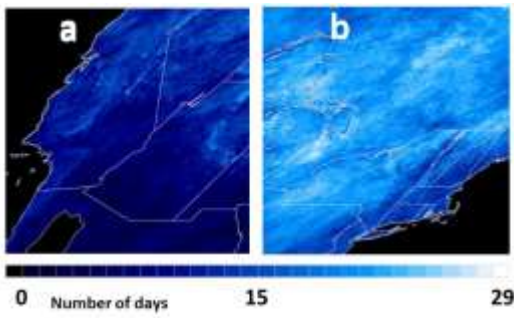
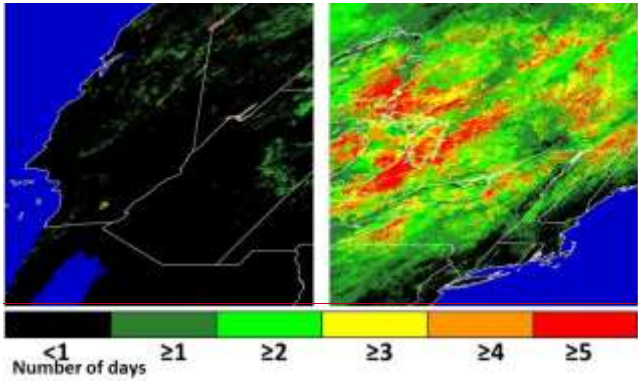
637 **4.3.3.12 Effect of cloud cover on the accuracy of the CGF snow-cover maps.**
638

Formatted: Font: Bold

Formatted: Font: Bold, Not Italic, No underline

Formatted: Font: Bold

639 The accuracy of the CGF snow decision in each pixel is influenced by cloud persistence, or the number of days of
640 continuous cloud cover. ~~This is because~~ the algorithm updates the snow map ~~under clear sky conditions, or~~ when
641 there are breaks in cloud cover, ~~according to~~ ~~as determined by~~ the MODIS or VIIRS cloud mask. To demonstrate
642 differences in cloud cover ~~age~~ and thus to illustrate ~~differences sources of~~ CGF uncertainty, between two
643 ~~climatologically different~~ areas ~~in the United States~~ ~~continental U.S.~~, we show the mean number of days of
644 ~~continuous~~ cloud cover for ~~an~~ ~~study~~ area in the western U.S./northern Mexico and in the northeastern
645 U.S./southeastern Canada for the month of February 2012 (Fig. 8a, b & c). Greater accuracy in snow-cover
646 decisions ~~in for~~ the CGF snow-cover product is ~~possible~~ ~~achieved~~ when there are more views of the surface as
647 ~~illustrated for in the month of February 2012; in~~ the western U.S./northern Mexico ROI (Fig. 8a) ~~are fewer days of~~
648 ~~clouds and more views of the surface (that includes the Sierra Nevada Mountains ROI discussed earlier) as~~
649 ~~compared to~~ ~~vs.~~ ~~in part of the~~ northeastern U.S./southeastern Canada (Fig. 8b). For example, for February 2012 the
650 mean number of days of continuous cloud cover on a per-grid-cell basis in the northeastern U.S./southeastern
651 Canada (2.67 days) is greater than in the western U.S./northern Mexico (0.49 days) as seen in Fig. 8b. Figs. 8a and
652 8b demonstrate graphically that there were more views of the surface in the western study area as compared to the
653 eastern study area for the month of February 2012. Thus the expectation is, that the accuracy of the CGF snow maps
654 at this time of year is higher in western U.S. study areas as compared to cloudier northeastern U.S. study areas.
655
656



657

658

659 **Figure 8a, b and c and 8b:** [Fig. 8a](#)—Maps showing the mean number of days of continuous cloud cover (a measure of cloud
 660 persistence) for February 2012 derived from the MOD35 cloud mask used in the MOD10A1F snow-cover products. [Fig. 8a](#)—A
 661 study area; [8a](#)) in the western U.S., extending into northern Mexico, and [8b](#)). [Fig. 8b](#)—A study area in the northeastern
 662 U.S./southeastern Canada. [Fig. 8c](#). [Location map](#) showing outlines, in red, the locations of the study areas shown in [Figs. 8a](#)
 663 and [8b](#).

664
665
666
667
668
669
670
671
672
673
674
675
676
677
678
679
680
681
682
683
684

4.3- Comparison of a time series of MODIS and VIIRS cloud-gap filled SCE maps

Formatted: Font: Bold

For the study area in the western U.S. shown in Figure 1, A ~3-month (14 February – 30 April, 2012) time series of Terra MODIS and S-NPP VIIRS SCE map products (Fig. 9) were developed, processed and evaluated for the study area in the western U.S. shown in Fig. 1. Note in Figure 9 the difference in SCE between the MODIS and VIIRS snow maps for each day of the time series is shown in the graph. Overall, the snow maps agree very well though the mean difference shows that in general, the Terra MODIS snow maps show more/less snow as compared to the VIIRS snow maps, with a mean daily difference of $-11,070 \text{ sq km}^2$, which represents only 0.45 percent of the study area which is only ~0.45 percent of the study area. Overall, the snow maps agree very well. Reasons for disagreement between MODIS and VIIRS on a given day/daily basis are that the Terra MODIS images are acquired at a different time of the day (10:30 A.M. equatorial crossing time) as compared to the S-NPP VIIRS images (1:30 P.M. equatorial crossing time); cloud-cover differences on the original snow maps (before gap filling) can also explain some of the difference in amount of snow mapped. This is largely because of differences in cloud masking between the MODIS and VIIRS SCE products as described earlier, in Section xx and as illustrated in the example shown in Fig. 2.

Formatted: Superscript

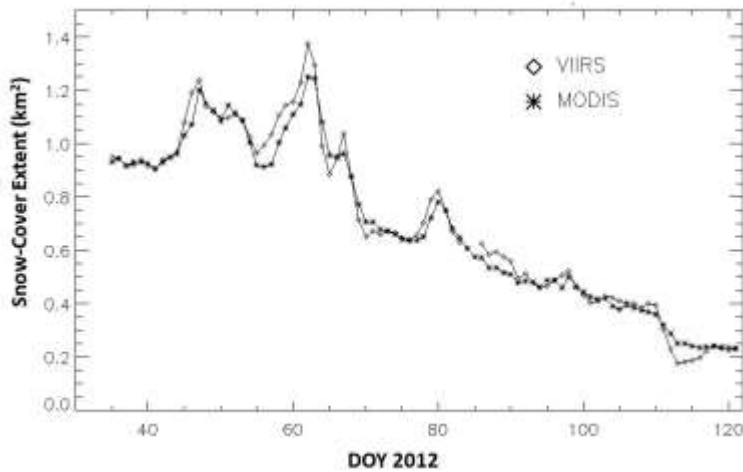
Formatted: Strikethrough, Highlight

Formatted: Font color: Auto, Strikethrough, Highlight

Formatted: Strikethrough, Highlight

Formatted: Font color: Red

Further analysis has confirmed that the differences in SCE between the two snow maps are largely due to differences in cloud masking.



685
686
687

Figure 9: Time series showing differences in snow-cover extent (SCE) derived from Terra MODIS and S-NPP VIIRS cloud-gap filled (CGF) snow maps for a nearly 3-month period extending from 4 February – 30 April, 2012. Though the time series began

Formatted: Font color: Auto

588 on 1 February, snow-cover extent from 1 – 3 February snow cover is not shown because, in this example, ~~xxx~~the gap-filling
589 algorithm was started on 1 February had not filled most of ~~in~~the gaps from clouds until 4 February.

Formatted: Font color: Auto

Formatted: Font color: Auto

Formatted: Font color: Auto

593 4.4 Development of Environmental Science Data Records using Cloud-Gap Filled Snow Maps

Formatted: Font: Bold

595 4.4.5.3.13 Comparison of Terra and Aqua MODIS snow maps for inclusion in an Earth Science Data Record 596 (ESDR).

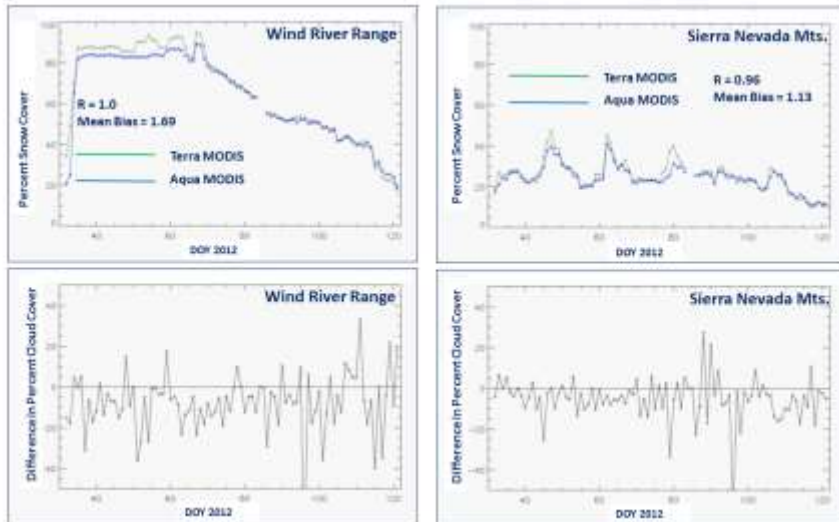
Formatted: Font: Bold, Not Italic, No underline

Formatted: Font: Bold, Not Italic, No underline

Formatted: Font: Bold

598 ~~Because of the greater uncertainties inherent in snow-mapping using MYD10 (Aqua) vs MOD10 (Terra) algorithms~~
599 ~~for reasons mentioned above that focus on Aqua band 6 issues, and because any combined method using both Terra~~
600 ~~and Aqua data is dependent on more than one sensor providing data, we do not recommend the Aqua MODIS SCE~~
601 ~~product to be part of a planned MODIS VIIRS ESDR for SCE.~~ We analyzed Terra and Aqua CGF snow maps and
602 time-series plots to determine which maps are better suited to being part of a moderate-resolution the SCE ESDR.
603 First we compared snow ~~maps map data~~ from both Terra and Aqua from 1 February through 30 April 2012 for ROIs
604 including the Wind River Range, Wyoming, and the Sierra Nevada Mountains in California and Nevada (see red
605 rectangles in Fig. 2, ~~left panels~~, for locations). In the first few days of each time series, the CGF algorithm is
606 actively removing clouds from the daily maps, until both the Terra and Aqua daily maps are completely cloud-free
607 by approximately DOY 20 of the Wind River Range ROI time series and Day 10 of the Sierra Nevada ROI time
608 series ~~as seen in Fig. 9~~. Pixels for which the algorithm provided “no decision” were excluded from the analysis.
609 The plots on the top row in Fig. 109 show ~~agreement of the Terra MODIS and Aqua CGF maps~~agreement of percent
610 snow cover as R=1.0, and Mean Bias=1.69 for the Wind River Range ROI time series and R=0.96 and Mean
611 Bias=1.13 for the Sierra Nevada ROI time series. ~~Difference in percent clouds in each ROI (in which the difference~~
612 ~~= Terra minus Aqua) reveals that the Aqua snow maps generally have more clouds than do the Terra snow maps.~~

614 ~~TEven when the “no decision” pixels are excluded, there are still differences in Terra and Aqua cloud masking that~~
615 ~~preclude prevent~~ the Terra and Aqua time series from being identical. This is especially notable from ~DOY 35 – 70
616 of the Wind River Range time series (see top left graph in Fig. 109). This corresponds to a period with significant
617 cloud cover that is being mapped differently by the Terra and Aqua cloud masks (see bottom row in Fig. 109).
618 Difference in percent cloud cover by day for Terra-MODIS minus Aqua CGF for the ROI including the Wind River
619 Range and the ROI including the Sierra Nevada Mountains are shown in the bottom row of Fig. 109. ~~TDifference in~~
620 ~~percent clouds in each ROI reveals that the Aqua snow maps generally have more clouds than do the Terra snow~~
621 ~~maps. The Aqua MODIS snow maps tends to have more cloud cover during the study period than does the Terra~~
622 ~~MODIS snow maps.~~



725
 726 **Figure 109:** Top Row. Time-series plots of percent snow cover in a 22,171 km² scene (see location of the ROI that includes the
 727 Wind River Range, Wyoming, in Fig. 2) and in a 109,575 km² scene (see ROI that includes the Sierra Nevada Mts., in Fig. 2)
 728 using M¹D10A1F snow-cover maps for a time series extending from 1 February through 30 April (DOY 32 – 121) 2012.
 729 Bottom Row. Difference in percent cloud cover by day for Terra MODIS minus Aqua MODIS for the ROI including the Wind
 730 River Range and the ROI including the Sierra Nevada Mountains, corresponding to the top panels, showing that the Aqua
 731 MODIS ~~has~~ shows more cloud cover during the study period than does the Terra MODIS.

732
 733 Though the percent snow cover on the Terra and Aqua snow maps is highly correlated in the ~~example~~ time series
 734 shown in Fig. 109, there is also quite a bit of disagreement for example from about DOY 35 – 70 for the Wind River
 735 Range. Our analysis of both CGF snow maps for this western U.S. study area indicates that the Terra MODIS snow
 736 maps are ~~is~~ superior for reasons that are as discussed for reasons described below. Further analysis, after the full
 737 dataset has been reprocessed, is required to confirm this.

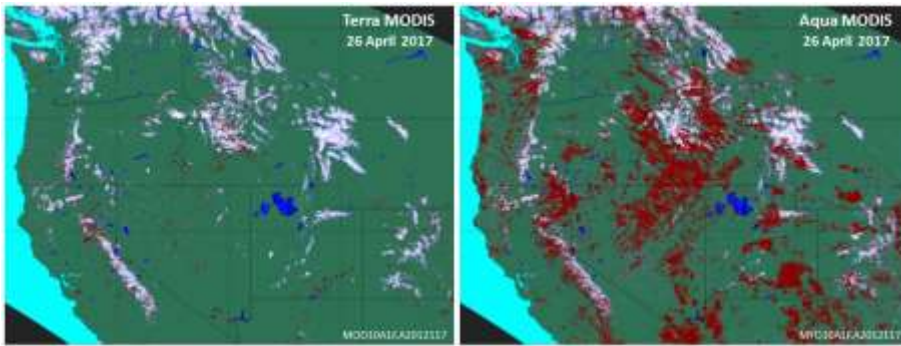
738
 739 The primary reason for disagreement between the Terra MODIS and Aqua MODIS snow maps in C5 and earlier
 740 collections is that the 1.6 μm channel (band 6) on the Aqua MODIS sensor has some non-functioning detectors
 741 (MCST, 2014) as described earlier. Other reasons include low illumination and terrain shadowing. The reader is
 742 referred to the MODIS C5 Snow Products User Guide (Riggs et al., 2004) for more details concerning the effect of
 743 the non-functioning detectors on the Aqua snow-cover maps in data collections prior to C6.

744
 745 For C6, the MYD10A1 snow-mapping algorithm uses the Quantitative Image Restoration (QIR) (of Gladkeova et
 746 al., 2012) to correct the Aqua MODIS band 6 radiances for the non-functioning detectors, and thereby to enable
 747 use of the same algorithm as is used for the Terra MODIS. Differences in cloud cover, and in cloud masking

748 account for differences in snow-mapping results between the C6 Terra and Aqua MODIS snow maps shown in Fig.
749 109. The lower panels in Fig. 109 illustrate differences in the cloud masking for Terra and Aqua for the 41-February
750 - 30-April 2012 time series.

751
752 An ~~specific~~ example to illustrate this can be seen on 26 April 2012 which was a day that had a large amount of
753 clouds in the ~~primary-western~~ U.S. study area ~~shown in Fig. 1 of the western United States~~ (Fig. 110). The
754 patterns of cloud cover in the false-color imagery (not shown) of both Terra and Aqua MODIS show that the clouds
755 ~~are in~~ have the same shape ~~of as~~ many of the 'no-decision' regions on the Aqua CGF snow map. The clouds are
756 probably very cold (possibly with ice) on top of lower-level clouds. The Aqua cloud mask fails to flag most of those
757 clouds as 'certain cloud,' so they are processed as 'clear' in the MYD10A1 snow algorithm, and 'no decision' is the
758 result. This is ~~an outcome of the fact that because the Aqua MODIS band 6 (with its non-functioning detectors) is~~
759 not used in the Aqua MODIS cloud masking algorithm ~~because of the non-functioning detectors~~. Even though
760 MYD10A1 uses the QIR for the C6 and C6.1 SCE algorithms, the C6 cloud masking algorithm, MYD35 developed
761 by the University of Wisconsin, does not "restore" the non-functioning detectors of Aqua band 6, and therefore
762 ~~uses Aqua band 7 instead~~.

763
764 This is a common problem with the C6 Aqua CGF snow maps, and ~~t~~he large number of 'no decision' pixels
765 resulting from the Aqua C6 and C6.1 cloud mask would affect the continuity of a moderate-resolution SCE n ESDR.
766 For that reason, we have decided to use of the Terra and VIIRS CGF maps only, as part of to develop the ESDR.
767



768
769 **Figure 110:** Terra MODIS (left) and Aqua MODIS (right) cloud-gap-filled (CGF) snow-cover maps from 26 April 2012. Note
770 that there are red pixels on both snow maps indicating 'no decision' by the algorithm, however there are many more red pixels on
771 the Aqua MODIS snow map, primarily due largely to the inability of the Aqua MODIS cloud mask to identify large areas of
772 cloud cover as 'certain cloud.' The location of this western United States study area is shown in Fig. 1.

773
774 There are greater uncertainties inherent in snow mapping using the Aqua MODIS vs. Terra MODIS for reasons
775 mentioned above that are largely related to the non-functioning detectors in the Aqua MODIS band 6. The large
776 number of 'no decision' pixels resulting from the Aqua C6 and C6.1 cloud mask would adversely affect the

777 ~~continuity of a moderate-resolution SCE ESDR. Based on this preliminary analysis, we recommend use of the Terra~~
778 ~~MODIS and S-NPP VIIRS CGF maps only, to develop the moderate-resolution SCE ESDR. Further analysis in~~
779 ~~other snow-covered areas is necessary to confirm this.~~

781 4.5 Development of Environmental Science Data Records using Cloud-Gap Filled Snow Maps

784 5.4 Discussion and Conclusion

787 Meltwater from mountain snowpacks provides hydropower and water resources to drought-prone areas such as the
788 western United States. Accurate snow measurement is needed as input to hydrological models that predict the
789 quantity and timing of snowmelt during spring runoff. SCE can be input to models to estimate snow-water
790 equivalent (SWE) which is the quantity of most interest to hydrologists and water management agencies.
791 Increasingly accurate predictions save money because reservoir management improves as measurement accuracy of
792 SWE increases.

794 In this paper, we describe ~~some of the applications and~~ some uncertainties of the C6.1 MODIS and VIIRS cloud-gap
795 filled (CGF) daily snow-cover maps, M*D10A1F and ~~the C2 the C22 VIIRS CGF snow-cover map,~~ VNP10A1F,
796 respectively. ~~The objective of this work the NASA MODIS and VIIRS algorithms products is to~~ produce a daily,
797 cloud-free snow-cover products along with appropriate QA information. ~~These products will enable that can SCE~~
798 can be used as the basis for that an Earth Science Data Record (ESDR) of snow cover to can be produced at moderate
799 spatial resolution for hydrological and climatological applications. Cloud-gap filled snow-cover products from
800 MODIS and VIIRS have all of the uncertainties of the original products, that contain clouds, as well as additional
801 uncertainties that are related to ~~cloud the age of the snow measurement gap filling, such as the age of the snow~~
802 observation method. When using the MODIS and VIIRS CGF products, a user can specify how far back in time
803 they want to look, using the Cloud-Persistence Count (CPC) which tells the age of the snow measurement in each
804 pixel; ~~the CPC, and~~ is available as part of the product QA metadata for both the MODIS and VIIRS CGF snow-
805 cover products. Uncertainty relating to cloud-gap filling is greater in areas with frequent and persistent cloud cover
806 during the snow season such as in the northeastern U.S. ~~or WRR vs.~~ areas such as the Sierra Nevada Mountains
807 where gaps in clouds occur more frequently during the snow season. ▲

809 It is difficult to validate the MODIS and VIIRS CGF (and other) snow maps. Absolute validation can only be
810 accomplished using ~~NOAA~~ daily snow depth station data when available. ~~However, pw~~ We can also evaluate the
811 product accuracy can also be evaluated by comparing the CGF ~~with MODIS products with~~ surface reflectance maps,
812 higher-resolution maps such as derived from Landsat and Sentinel and using other satellite-derived snow maps.

Formatted: Not Highlight

Formatted: Not Highlight

Formatted: Not Highlight

Formatted: Font color: Auto

Formatted: Font: Italic

814 Comparisons of the daily MODIS and VIIRS CGF SCE products for a nearly 3-month time period in 2012 over a
815 study area in the western U.S. (2,487,610 km²) show excellent correspondence between the products with the VIIRS
816 products, on average, mapping 11,070 km² more snow as compared to the MODIS products on a given day, or 0.45
817 percent of the study area.

Formatted: Font color: Red

Formatted: Font color: Red

Formatted: Font color: Red

Formatted: Font: 10 pt

Formatted: Normal

818 ▲
819 Comparisons of Terra and Aqua CGF snow maps in C6 reveal many more “no-decision” pixels in the Aqua snow
820 maps, due to cloud masking, low illumination and terrain shadowing. Because of non-functioning detectors in band
821 6, the Aqua cloud mask is less accurate than the Terra cloud mask according to our preliminary validation over the
822 western U.S. study area. Though the Terra and Aqua snow algorithms are the same in C6 due to use of the
823 Quantitative Image Restoration (QIR) technique technique to map snow using for the Aqua MODIS, the Aqua cloud
824 mask does not use the QIR but the accuracy of the Terra product is higher, and therefore the Terra- MODIS CGF
825 snow-cover maps of C6.1 are useful for development of an ESDR and ultimately a CDR (combined with S-NPP
826 VIIRS and other JPSS VIIRS-derived snow maps now and in the future).

Formatted: Highlight

827
828 Time-series of both the Terra and Aqua daily CGF snow-cover maps show pixels classified as ‘no decision,’ but on
829 the Aqua CGF maps, there are many more ‘no decision’ pixels on the Aqua maps. Because of this issue with the
830 Aqua-MODIS cloud masking, as detailed above, ThereforeFor this reason we do not recommend using the C6.1
831 Aqua-MODIS CGF snow maps as part of an ESDR at this time. In the future, if the Terra and Aqua cloud-mask
832 algorithms become more similar in future re-processing of the cloud mask, this recommendation will be reassessed.

833
834 Comparisons of the daily Terra MODIS and S-NPP VIIRS CGF SCE products for a 3-month time period in 2012
835 were undertaken for our study area in the western U.S. (2,487,610 km²) covering all or parts of 11 states and part of
836 southwest Canada. Though the MODIS and VIIRS SCE maps show excellent correspondence, the VIIRS maps, on
837 average, show 11,070 km² more snow as compared to the MODIS maps on a given day which is only ~0.45
838 percent of the study area. MODIS CGF snow-cover maps of C6.1 are useful for development of an ESDR and
839 ultimately a CDR (combined with S-NPP VIIRS and other JPSS VIIRS-derived snow maps now and in the future).

Formatted: Font color: Auto

Formatted: Font color: Auto

Formatted: Not Highlight

840
841
842
843 Snow cover is one of the Global Climate Observing System (GCOS) essential climate variables. The distribution,
844 extent and duration of snow, along with knowledge of snowmelt timing, are critical for characterizing the Earth’s
845 climate system and its changes. To augment-complement the 53-year NOAA/Rutgers CDR of snow cover at 25-km
846 resolution which is valuable for climate and other studies, the MODIS/VIIRS moderate-resolution ESDR will be
847 available at 500-m resolution and as such will be useful for local and regional studies of snow cover and water
848 resources, as well as for climate studies. The value of the ESDR will increase as- as the length of the record
849 increases.

850

851 **Acknowledgements**

852

853 We would like to acknowledge support from NASA's Terrestrial Hydrology (grant # 80NSSC18K1674) and Earth
854 Observing Systems programs (grant # NNG17HP01C). The *Sentinel-2A* satellite is operated by the European Space
855 Agency (ESA); a collaborative effort between ESA and the USGS provides a data portal for Sentinel-2A data
856 products.

857

858 **References**

859

860 Arsenault, K. R., Houser, P. R., and De Lannoy, G. J.: Evaluation of the MODIS snow cover fraction product,
861 *Hydrological Processes*, 28(3), 980-998, 2014.

862

Brubaker, K. L., Pinker, R.T., and Deviatova, E: Evaluation and Comparison of MODIS and IMS Snow-Cover
Estimates for the Continental United States Using Station Data, *Journal of Hydrometeorology*, 6(6), 1002-1017,
2005.

863

864 Chelamallu, H.P., Venkataraman G., and Murti, M.V.R.: Accuracy assessment of MODIS/Terra snow cover product
865 for parts of Indian Himalayas, *Geocarto International*, 29(6), 592-608, 2013.

866

867 Chen, C., Lakhankar, T., Romanov, P., Helfrich, Powell, A., and Khanbilvardi, R.: Validation of NOAA-interactive
868 multisensor snow and ice mapping system (IMS) by comparison with ground-based measurements over continental
869 United States, *Remote Sensing* 4(5), 1134-1145, 2012.

870

871 Claverie, M., Ju, J., J.G. Masek, J.G., Dungan, J.L., Vermote, E.F., Roger, J.-C., Skakun, S.V., and C. Justice, C.:
872 The Harmonized Landsat and Sentinel-2 surface reflectance data set, *Remote Sensing of Environment*, 219, 145-
873 161, 2018.

874

875 Coll, J. and Li, X.: Comprehensive accuracy assessment of MODIS daily snow cover products and gap filling
876 methods, *ISPRS Journal of Photogrammetry and Remote Sensing*, 144, 435-452, 2018.

877

878 Crawford, C.J.: MODIS Terra Collection 6 fractional snow cover validation in mountainous terrain during spring
879 snowmelt using Landsat TM and ETM+, *Hydrological Processes*, 29(1), 128-138, 2015.

880

881 Dariane, A. B., Khoramian, A., and Santi, E. Investigating spatiotemporal snow cover variability via cloud-free
882 MODIS snow cover product in Central Alborz Region, *Remote sensing of Environment*, 202, 152-165, 2017.

883

884 Deng, J., Huang, X., Feng, Q., Ma, X., and Liang, T.: Toward improved daily cloud-free fractional snow cover
885 mapping with multi-source remote sensing data in China, *Remote Sensing*, 7, 6986-7006, 2015.

886

887 Déry, S.J. and Brown, R.D.: Recent Northern Hemisphere snow cover extent trends and implications for the snow-
888 albedo feedback, *Geophysical Research Letters*, 34, L22504, 2007.

889

890 Dietz, A.J., Kuenzer, C., and Conrad, C.: Snow-cover variability in central Asia between 2000 and 2011 derived
891 from improved MODIS daily snow-cover products, *International Journal of Remote Sensing*, 34(11), 3879-3902,
892 <https://doi.org/10.1080/01431161.2013.767480>, 2013.

893

Dong, C. and Menzel, L.: Producing cloud-free MODIS snow cover products with conditional probability
interpolation and meteorological data, *Remote Sensing of Environment*, 186, 439-451,
<https://doi.org/10.1016/j.rse.2016.09.019>, 2016.

894

Estilow, T.W., Young, A.H., and Robinson, D.A.: A long-term Northern Hemisphere snow cover extent data record
for climate studies and monitoring, *Earth System Science Data*, 7, 137-142, 2015.

Foppa, N. and Seiz, G.: Inter-annual variations of snow days over Switzerland from 2000-2010 derived from
MODIS satellite data, *The Cryosphere*, 6, 331-342, 2012.

895 [Foster, J.L., Hall, D.K., Eylander, J. B., Riggs, G.A., Nghiem, S.V., Tedesco, M., Kim, E. et al.: A blended global](#)
896 [snow product using visible, passive microwave and scatterometer satellite data, International Journal of Remote](#)
897 [Sensing, 32\(5\), 1371-1395, 2011.](#)

Frei, A. and Lee, S.: A comparison of optical-band based snow extent products during spring over North America,
Remote Sensing of Environment, 114, 1940-1948, 2010.

898

Gafurov, A. and Bardossy, A.: Cloud Removal Methodology from MODIS Snow Cover Product, *Hydrology and*
Earth System Sciences, 13, 1361-1373, 2009.

Gafurov, A., Lütke, S., Unger-Shayesteh, K., Vorogushyn, S., Schöne, T., Schmidt, S., Kalashnikova, O., and
Merz, B.: MODSNOW-Tool: an operational tool for daily snow cover monitoring using MODIS data,
Environmental Earth Sciences, 75, 1078, 2016.

899 Gao, Y., Xie, H., Yao, T., and Xue, C.: Integrated assessment on multi-temporal and multi-sensor combinations for
900 reducing cloud obscuration of MODIS snow cover products of the Pacific Northwest USA, *Remote Sensing of*
901 *Environment*, 114(8), 1662-1675, 2010.

Formatted: Font: 10 pt

Formatted: Font: 10 pt

Formatted: Font: 10 pt

Formatted: Font: 10 pt

Formatted: Widow/Orphan control, Don't suppress line numbers, Hyphenate, Tab stops: Not at 0.64" + 1.27" + 1.91" + 2.54" + 3.18" + 3.82" + 4.45" + 5.09" + 5.73" + 6.36" + 7" + 7.63" + 8.27" + 8.91" + 9.54" + 10.18"

Formatted: Font: 10 pt

Formatted: Font: 10 pt

Formatted: Font: 10 pt

Formatted: Font: Not Italic

Formatted: Font: 10 pt, Not Italic

Formatted: Font: Not Italic

Formatted: Font: 10 pt

Formatted: Font: 10 pt

Formatted: Font:

902
903 Gao, Y., Xie, H., Lu, N., Yao, T., and Liang, T., 2010. Toward advanced daily cloud-free snow cover and snow
904 water equivalent products from Terra–Aqua MODIS and Aqua AMSR-E measurements, *J. Hydrol.*, 385, 23–35,
905 <https://doi.org/10.1016/j.jhydrol.2010.01.022>, 2010.

906
907
908 ~~Maybe add this:~~ Gao, Y., Lu, N., and Yao, T.: Evaluation of a cloud-gap-filled MODIS daily snow cover product
909 over the Pacific Northwest USA. *J. Hydrol.*, 404, 157–165, <https://doi.org/10.1016/j.jhydrol.2011.04.026>, 2011.

910
911 Gladkova, I., Grossberg, M., Bonev, G., Romanov, P., and Shahriar, F.: Increasing the accuracy of MODIS/Aqua
912 snow product using quantitative image restoration technique, *IEEE Geoscience and Remote Sensing Letters*, 9(4),
913 740-743, 2012.

914
915 ~~Not in paper:~~ Hall, D.K., Riggs, G.A., Salomonson, V.V., DiGirolamo, N.E., and Bayr, K.J.: MODIS Snow Cover
916 Products, *Remote Sensing of Environment*, 83(1-2), 181-194, 2002.

917
918 Hall, D.K. and Riggs, G.A.: Accuracy Assessment of the MODIS Snow Products, *Hydrological Processes*, 21(12),
919 1534-1547, 2007.

920
921 Hall, D.K., Riggs, G.A., Foster, J.L. and Kumar, S.V.: Development and evaluation of a cloud-gap-filled MODIS
922 daily snow-cover product, *Remote Sensing of Environment*, 114, 496-503, <https://doi.org/10.1016/j.rse.2009.10.007>,
923 2010.

924
925 Hall, D. K., Crawford, C. J., DiGirolamo, N. E., Riggs, G. A., and Foster, J. L.: Detection of earlier snowmelt in the
926 Wind River Range, Wyoming, using Landsat imagery, 1972–2013, *Remote Sensing of Environment*, 162, 45-54,
927 2015.

928
929 Hammond, J.C., Saavedra, F.A., and Kampf, S.K.: Global snow zone maps and trends in snow persistence 2001-
930 2016, *International Journal of Climate*, 38(12), 4369-4383, <https://doi.org/10.1002/joc.5674>, 2018.

931
932 Helfrich, S.R., McNamara, D., Ramsay, B.H., Baldwin, T., and Kasheta, T.: Enhancements to, and forthcoming
933 developments in the Interactive Multisensor Snow and Ice Mapping System (IMS), *Hydrological processes* 21(12),
934 1576-1586, 2007.

935
936 Helfrich, S. R., Li, M., and Kongoli, C.: Interactive Multisensor Snow and Ice Mapping System Version 3 (IMS V3)
937 Algorithm Theoretical Basis Document Version 2.0 Draft 4.1., NOAA NESDIS Center for Satellite Applications
938 and Research (STAR), 2012.

939

Huang, X., Liang, T., Zhang, X., and Guo, Z.: Validation of MODIS snow cover products using Landsat and ground measurements during the 2001-2005 snow seasons over northern Xinjiang, China, *International Journal of Remote Sensing*, 32(1):133 -152, 2011.

~~Not found in paper: Hüsler, F., Jonas, T., Riffler, M., Musial, J.P., and Wunderle, S.: A satellite-based snow cover climatology (1985-2011) for the European Alps derived from AVHRR data, *The Cryosphere*, 8, 73-90, 2014.~~

Kadlec, J. and Ames, D.P.: Using crowdsources and weather station data to fill cloud gaps in MODIS snow cover datasets, *Environmental Modelling and Software*, 95, 258-270, 2017.

940

941 Klein, A.G., and Barnett, A.C.: Validation of daily MODIS snow cover maps of the Upper Rio Grande River Basin
942 for the 2000–2001 snow year, *Remote Sensing of Environment*, 86(2), 162-176.

943

944 Li, X., Fu, W., Shen, H., Huang, C., and Zhang, L.: Monitoring snow cover variability (2000–2014) in the
945 Hengduan Mountains based on cloud-removed MODIS products with an adaptive spatio-temporal weighted method,
946 *Journal of Hydrology*, <https://doi.org/10.1016/j.jhydrol.2017.05.049>, 2017

947

948 López-Burgos, V., Gupta, H.V., and Clark, M.: Reducing cloud obscuration of MODIS snow cover area products by
949 combining spatio-temporal techniques with a probability of snow approach, *Hydrology and Earth System Sciences*,
950 17, 1809-1823, 2013.

951

952 MCST, 2014: MODIS Characterization Support Team, Website: <https://mcst.gsfc.nasa.gov>.

953

954 Malnes, E., Karlsen, S.R., Johansen, B., Bjerke, J.W., and Tømmervik, H.: Snow season variability in a boreal-
955 Arctic transition area monitored by MODIS data, *Environmental Research Letters*, 11, 125005, 2016.

956

957 Matson, M. and Wiesnet, D.R.: New database for climate studies, *Nature*, 289, 451-456, 1981.

958

959 Mote, P.W., Hamlet, A.F., Clark, M.P., and Lettenmaier, D.P.: Declining mountain snowpack in western North
960 America, *Bulletin of the American Meteorological Society*, 86(1), 39–49, 2005.

961

962 O’Leary, D., Hall, D., Medler, M., and Flower, A.: Quantifying the early snowmelt event of 2015 in the Cascade
963 Mountains, USA by developing and validating MODIS-based snowmelt timing maps, *Frontiers of Earth Science*,
964 12(4), 693-710, 2018.

965

966

967 ~~Not found in text:~~ Parajka, J. and G. Blöschl, 2006: Validation of MODIS snow cover images over Austria,
968 *Hydrology and Earth System Sciences*, 10(5), 679-689.

969

970 Parajka, J. and Blöschl, G.: Spatio-temporal combination of MODIS images–potential for snow cover mapping,
971 *Water Resources Research*, 44(3), 2008.

972

973 Parajka, J., Pepe, M., Rampini, A., Rossi, S., and Blöschl, G.: A regional snow-line method for estimating snow
974 cover from MODIS during cloud cover, *Journal of Hydrology*, 381(3-4), 203-212, 2010.

975

976 Parajka, J., Holko, L., Kostka, Z., and Blöschl, G.: MODIS snow cover mapping accuracy in a small mountain
977 catchment–comparison between open and forest sites, *Hydrology and Earth System Sciences*, 16(7), 2365-2377,
978 2012.

979

980 Paudel, K.P. and Anderson, P.: Monitoring snow cover variability in an agropastoral area in the Trans Himalayan
981 region of Nepal using MODIS data with improved cloud removal methodology, *Remote Sensing of Environment*,
982 115(5), 1234–1246, 2011.

983

984 ~~Not found in paper:~~ Riggs, G.A., Hall, D.K., and Salomonson, V.V.: MODIS Snow Products User Guide to
985 [Collection 5, https://modis-snow-ice.gsfc.nasa.gov/?c=userguides](https://modis-snow-ice.gsfc.nasa.gov/?c=userguides), 2006.

986

987 Riggs, G.A., Hall, D.K., and Román, M.O.: Overview of NASA’s MODIS and Visible Infrared Imaging Radiometer
988 Suite (VIIRS) snow-cover, *Earth Syst. Sci. Data*, 9, 1–13, <https://www.earth-syst-sci-data.net/9/765/2017/>, 2017a.

989

990 [Riggs, G.A., Hall, D.K., and Román, M.O.: NASA S-NPP VIIRS Snow Products Collection 1 \(C1\) User Guide,](https://modis-snow-ice.gsfc.nasa.gov/?c=userguides)
991 [Release 1.0, https://modis-snow-ice.gsfc.nasa.gov/?c=userguides](https://modis-snow-ice.gsfc.nasa.gov/?c=userguides), 2017b.

992

993 Riggs, G.A., D.K. Hall, D.K., and Román, M.O.: MODIS snow products user guide for Collection 6.1 (C6.1),
994 available at: <https://modis-snow-ice.gsfc.nasa.gov/?c=userguides>, last accessed: 3/17/2019, 2018.

995

996 Robinson, D.A., Dewey, K.F., and Heim, R.R.: Global snow cover monitoring: An update, *Bull. Am. Meteorol.*
997 *Soc.*, 74, 1689–1696, 1993.

998

999 Salomonson, V.V. and Appel, I.: Estimating fractional snow cover from MODIS using the normalized difference
1000 snow index, *Remote Sensing of Environment*, 89(3), 351-360, 2004.

1001

1002 [Salomonson, V.V. and Appel, I., Development of the Aqua MODIS NDSI fractional snow cover algorithm and](https://doi.org/10.1109/JGRS.2006.1174717)
1003 [validation results, IEEE Transactions on Geoscience and Remote Sensing, 44\(7\), 1747-1756, 2006.](https://doi.org/10.1109/JGRS.2006.1174717)

- Formatted: Font: 10 pt
- Formatted: Font: 10 pt
- Formatted: Line spacing: 1.5 lines
- Formatted: Font: 10 pt
- Formatted: Font: 10 pt
- Formatted: Font: 10 pt, Not Italic
- Formatted: Font: 10 pt, Not Italic
- Formatted: Font: 10 pt, Not Italic
- Formatted: Font: 10 pt, Not Italic
- Formatted: Font: 10 pt
- Formatted: Font: 10 pt, Not Italic
- Formatted: Font: 10 pt
- Formatted: Font: 10 pt
- Formatted: Font: 10 pt

1004
1005
1006 Stewart, I.T.: Changes in snowpack and snowmelt runoff for key mountain regions, *Hydrological Processes*, 23(1),
1007 78–94, 2009.
1008
1009 Tang, Z., Wang, J., Li, H., and Yan, L.: Spatiotemporal changes of snow cover over the Tibetan plateau based on
1010 cloud-removed moderate resolution imaging spectroradiometer fractional snow cover product from 2001 to 2011,
1011 *Journal of Applied Remote Sensing*, 7(1), 073582, 2013.
1012
1013 Tang, Z., Wang, X., Wang, J., Wang, X., Li, H., and Jinag, Z.: Spatiotemporal variation of snow cover in Tianshan
1014 Mountains, Central Asia, based on cloud-free MODIS fractional snow cover product, 2001-2015, *Remote Sensing*,
1015 9(10), 1045, 2017.
1016
1017 Thompson, J.A., Paull, D.J. and Lees: An improved liberal cloud-mask for addressing snow/cloud confusion with
1018 MODIS, *Photogramm. Eng. Rem. Sens.*, 81, 19-29, 2015
1019
1020 Tong, J., Déry, S.J., and Jackson, P.L.: Topographic control of snow distribution in an alpine watershed of western
1021 Canada inferred from spatially-filtered MODIS snow products, *Hydrology and Earth System Sciences*, 13(3), 319-
1022 326, 2009a.
1023
1024 Tong, J., Déry, S.J., and Jackson, P.L.: Interrelationships between MODIS/Terra remotely sensed snow cover and
1025 the hydrometeorology of the Quesnel River Basin, British Columbia, Canada, *Hydrology and Earth System*
1026 *Sciences*, 13(8), 1439-1452, 2009b.
1027
1028 Westerling, A.L., Hidalgo, H.G., Cayan, D.R., and Swetnam, T.W.: Warming and earlier spring increase western
1029 U.S. forest wildfire activity, *Science*, 313(5789), 940, 2006.
1030
1031 Yu, J., Zhang, G., Yao, T., Xie, H., Zhang, H., Ke, C., and Yao, R.: Developing daily cloud-free snow composite
1032 products from MODIS Terra-Aqua and IMS for the Tibetan Plateau, *IEEE Trans. on Geosci. and Remote Sensing*,
1033 54(4), 2171- 2180, 2016.
1034
1035 Xu, W., Ma, H., Wu, D., and Yuan, W.: Assessment of the Daily Cloud-Free MODIS Snow-Cover Product for
1036 Monitoring the Snow-Cover Phenology over the Qinghai-Tibetan Plateau, *Remote Sensing* 9(6), 585,
1037 <https://doi:10.3390/rs9060585>, 2017.